# NAVAL POSTGRADUATE SCHOOL
## Monterey, California


# THESIS

**EXPERIMENTAL STUDIES OF NOISE/VIBRATION DAMPING FOR UNDERSEA WARFARE APPLICATIONS**

by

John J. Cahill

June 2002

Thesis Advisor: Y. S. Shin

**Approved for public release; distribution is unlimited.**

THIS PAGE INTENTIONALLY LEFT BLANK

| REPORT DOCUMENTATION PAGE | | | Form Approved OMB No. 0704-0188 |
|---|---|---|---|
| Public reporting burden for this collection of information is estimated to average 1 hour per response, including the time for reviewing instruction, searching existing data sources, gathering and maintaining the data needed, and completing and reviewing the collection of information. Send comments regarding this burden estimate or any other aspect of this collection of information, including suggestions for reducing this burden, to Washington headquarters Services, Directorate for Information Operations and Reports, 1215 Jefferson Davis Highway, Suite 1204, Arlington, VA 22202-4302, and to the Office of Management and Budget, Paperwork Reduction Project (0704-0188) Washington DC 20503. | | | |
| **1. AGENCY USE ONLY** ***(Leave blank)*** | **2. REPORT DATE** June 2001 | **3. REPORT TYPE AND DATES COVERED** Master's Thesis | |
| **4. TITLE AND SUBTITLE**: Title (Mix case letters) Experimental Studies of Noise/Vibration Damping for Undersea Warfare Applications | | | **5. FUNDING NUMBERS** |
| **6. AUTHOR(S) John J Cahill** | | | |
| **7. PERFORMING ORGANIZATION NAME(S) AND ADDRESS(ES)** Naval Postgraduate School Monterey, CA 93943-5000 | | | **8. PERFORMING ORGANIZATION REPORT NUMBER** |
| **9. SPONSORING /MONITORING AGENCY NAME(S) AND ADDRESS(ES)** N/A | | | **10. SPONSORING/MONITORING AGENCY REPORT NUMBER** |
| **11. SUPPLEMENTARY NOTES** The views expressed in this thesis are those of the author and do not reflect the official policy or position of the Department of Defense or the U.S. Government. | | | |
| **12a. DISTRIBUTION / AVAILABILITY STATEMENT** Approved for public release; distribution is unlimited. | | | **12b. DISTRIBUTION CODE** |

**13. ABSTRACT** ***(maximum 200 words)***

Maintaining silence underwater is an important issue with undersea warfare. One technique to reduce noise radiation is to use a passive noise/vibration material. The objective of this research was to investigate the vibration properties of an aluminum foam with various types of damping treatment. The importance of the determination of the damping properties of the aluminum foam and various damping treatments was for the future development of materials that would reduce the radiated noise of undersea weapons and onboard machinery. The frequency response was determined using three tests; swept sine, impact hammer, and random noise. The natural frequencies were determined by examining the Nyquist plot of the frequency response. The damping ratios were determined by using the half-power point method.

| **14. SUBJECT TERMS** vibration, damping, constrained viscoelastic layer, viscoelastic damping, noise | | | **15. NUMBER OF PAGES** 75 |
|---|---|---|---|
| | | | **16. PRICE CODE** |
| **17. SECURITY CLASSIFICATION OF REPORT** Unclassified | **18. SECURITY CLASSIFICATION OF THIS PAGE** Unclassified | **19. SECURITY CLASSIFICATION OF ABSTRACT** Unclassified | **20. LIMITATION OF ABSTRACT** UL |

NSN 7540-01-280-5500 Standard Form 298 (Rev. 2-89)
Prescribed by ANSI Std. 239-18

THIS PAGE INTENTIONALLY LEFT BLANK

**Approved for public release; distribution is unlimited.**

# EXPERIMENTAL STUDIES OF NOISE/VIBRATION DAMPING FOR UNDERSEA WARFARE APPLICATIONS

John J Cahill
Ensign, United States Navy
B.S.M.E, University of Florida, 2001

Submitted in partial fulfillment of the
requirements for the degree of

**MASTER OF SCIENCE IN MECHANICAL ENGINEERING**

from the

**NAVAL POSTGRADUATE SCHOOL**
**June 2002**

Author: _____
John J. Cahill

Approved by: _____
Young S. Shin
Thesis Advisor

_____
Terry R. McNelley
Chairman, Department of Mechanical Engineering

THIS PAGE INTENTIONALLY LEFT BLANK

# ABSTRACT

Maintaining silence underwater is an important issue with undersea warfare. One technique to reduce noise radiation is to use a passive noise/vibration material. The objective of this research was to investigate the vibration properties of an aluminum foam with various types of damping treatment. The importance of the determination of the damping properties of the aluminum foam and various damping treatments was for the future development of materials that would reduce the radiated noise of undersea weapons and onboard machinery. The frequency response was determined using three tests; swept sine, impact hammer, and random noise. The natural frequencies were determined by examining the Nyquist plot of the frequency response. The damping ratios were determined by using the half-power point method.

THIS PAGE INTENTIONALLY LEFT BLANK

# TABLE OF CONTENTS

THIS PAGE INTENTIONALLY LEFT BLANK

# LIST OF FIGURES

# LIST OF TABLES

THIS PAGE INTENTIONALLY LEFT BLANK

# ACKNOWLEDGMENTS

The author would like to extend sincere thanks and gratitude to Professor Young S. Shin for his guidance. Additionally, the author would like to thank Dr. Chanman Park for his assistance in the making of the viscoelastic-aluminum foam composite. Also, the author would like to thank Tom Christian for his help in with the laboratory equipment and experimental setup for the research. The author would also like to thank Professor Joshua Gordis for his help in learning on how to operate all the test equipment.

THIS PAGE INTENTIONALLY LEFT BLANK

# I. INTRODUCTION

## A. BACKGROUND

Undersea warfare is based on maintaining silence in the water. Noise from equipment such as engines and onboard machinery are major sources of radiated noise from undersea vehicles and weapons. Passive methods for vibration control have proven to be an effective way to reduce the radiated noise. A lightweight material with high damping properties can provide the solution for reducing the noise/vibration from undersea vehicles and weapons. Aluminum foams are an ultra-light, functional material that can be used for sound absorption [Ref. 1].

The damping characteristics of the aluminum foam can be increased using a number of techniques. Viscoelastic-aluminum foam composite and a constrained viscoelastic layer are just two examples of increasing the damping of the aluminum foam. Both are effective ways to increase the damping of materials but problems arise with predicting the effectiveness of each method. The inverse homogenization approach can be a good candidate in designing composites with specially tailored properties. In this approach, composites are assumed to have periodic microstructures [Ref. 2]. Another technique proposed by M. P. Bendsoe and N. Kikuchi assumes the microstructure configuration of a composite is represented by a density distribution in the unit cell. Then, an optimal density distribution is sought so that the resulting composite exhibits the prescribed or optimal effective material properties [Ref. 3, 4]. Unfortunately, research on the vibration properties of the aluminum foam are limited, therefore experimental methods in determining the vibration characteristics are necessary.

Efforts have been made to predict the vibration characteristics of a material using a constrained viscoelastic layer to increase damping. Finite element models using classical and layer-wise laminate theory attempt to predict the response of such materials. [Ref. 5]. Another method, developed by Johnson and Kienholz, is a finite element technique that uses the Modal Strain Energy (MSE). MSE uses the structural strain energy to approximate the damping of the structure with an applied constrained viscoelastic damping system. [Ref 6, 7]. All methods have proven to predict vibration

responses of materials using a constrained viscoelastic layer accurately, but similar to the viscoelastic-aluminum foam composite, the research of the aluminum foam is limited and experimental methods must be used to determine the vibration properties.

## B. OBJECTIVES

The objective of this research is to investigate the vibration properties of the aluminum alloy foam with two types of damping treatments. The importance of the study of the vibration damping properties is for the future development of materials that could be used to reduce the radiated noise from underwater weapons and onboard machinery. The material should be lightweight and have a high stiffness while possessing high damping.

The two damping treatments used were a constrained viscoelastic layer on the surface of the aluminum foam and a viscoelastic material cured to form a composite with the aluminum foam as the composite matrix. Testing of the damping treatments was conducted to determine the effectiveness in increasing the damping ratio while maintaining a low weight density and a high material stiffness.

## C. MATERIAL DESCRIPTION

One of the objectives was to design a material with high damping characteristics while having a low weight density and high stiffness. The material proposed is an aluminum alloy foam. The aluminum alloy foam can be manufactured with a porosity varying from 5 to 40 pores per inch (ppi). The weight density of the aluminum alloy foam can be manufactured with a varying density of 3-10% the weight density of the original base material. The aluminum foam is available in 6101 and A-356 aluminum alloy while other aluminum alloys are available upon special request.

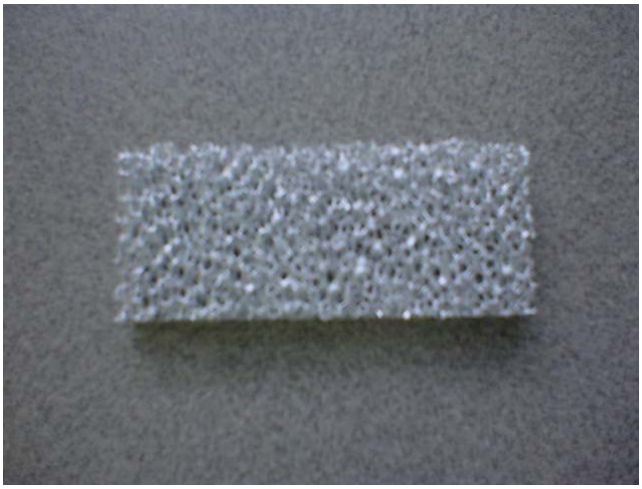

Figure 1. 10-ppi, 6101 aluminum alloy foam [Ref. 8]

Companies such as Cymat Corp and ERG Materials and Aerospace Corporation manufacture the aluminum alloy foam. The aluminum foam can be manufactured and shaped into various forms to suit the application. Complex shapes can be formed by using the investment casting process and the 3-D woven technique.

In investment casting, polymer foam is used as a starting point. The open pores are formed in the polymer foam by manipulating the foaming process or by a reticulation treatment. The polymer foam is then filled with a slurry of refractory material such as phenolic resin or calcium carbonate. The polymer is then vaporized to leave an open pore mould for the metal. Once the aluminum has been formed in the mould, the refractory material is removed and the aluminum foam is formed. The investment casting process is ideal for metals with low melting points, such as copper, lead, zinc, tin, and aluminum alloys. The aluminum foam can be formed using special machine-shop equipment to manufacture different shapes.

The 3-D woven technique is another method in creating the aluminum foam. The aluminum foam made in this technique can be more easily controlled resulting in more regular shapes than in the previous technique. Figure 2 is a sample of the various shapes the aluminum foam can be formed.

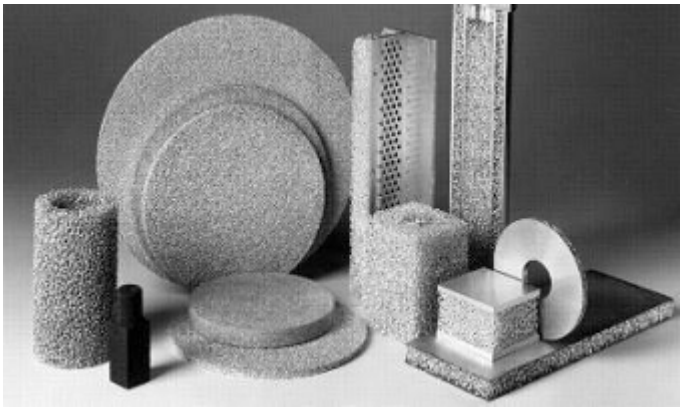

Figure 2. Various shapes of the aluminum foam [From Ref. 8]

The aluminum foam has been used in industry since 1968 in a number of applications. The aluminum foam can be used in fluid flow conditioning. Some fluid flow conditioning applications include uniform gas distribution, orifice flow stabilization, and contamination filtration and condensation. Because of the high specific surface area the pressure drop can be controlled for a fluid stream. Figure 3 shows the air pressure drop versus airflow for various aluminum foam ppi.

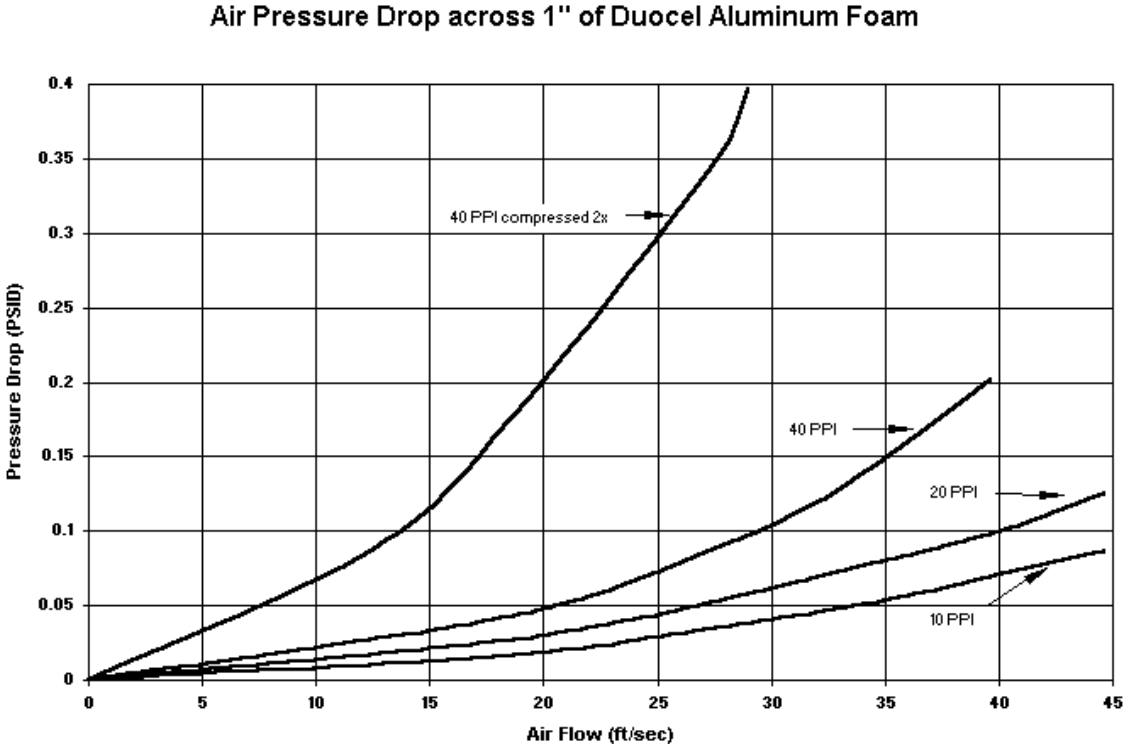


Figure 3. Air pressure drop across 1-inch of aluminum foam [From Ref. 8]

The aluminum foam has also been used in heat exchangers. The aluminum foam has a similar conductivity as the base alloy material with the advantage of a low weight density. This makes the aluminum foam ideal for aerospace applications were weight is a factor. Figure 4 shows the aluminum foam used to increase the surface area of a heat pump in a solar powered, non-polluting air conditioner.


Figure 4. Heat pump in a solar powered, non-polluting air conditioner [From Ref. 8]

Other applications of the aluminum foam include the following:

- Heat Shielding for aircraft exhaust
- Battery plates and spacers
- Aircraft wing structure
- Porous electrodes
- Race car deformable structure
- Catalyst surfaces

Not much in the way of noise/vibration reduction has been done for the aluminum foam. This research is intended to investigate the effectiveness of the aluminum foam with varies damping treatments in noise/vibration reduction applications.

The material damping was increased using two different methods. The first method to increase the damping was to use a viscoelastic material poured over the aluminum foam to form a composite material. The aluminum foam used in the composite was a 10-ppi, quarter-inch 6101 aluminum alloy foam. Diamont Coating Systems [Ref. 9] produces the viscoelastic material used for the composite. The average thickness of the

material was 0.270 inches and had a weight of 1.36 lbs. Figure 5 was the composite material used in the test.


Figure 5. The viscoelastic-aluminum foam composite

The other method used to increase the damping of the aluminum foam was to use a constrained viscoelastic layer. Figure 6 shows how the constrained viscoelastic layer was applied to the surface of the material.

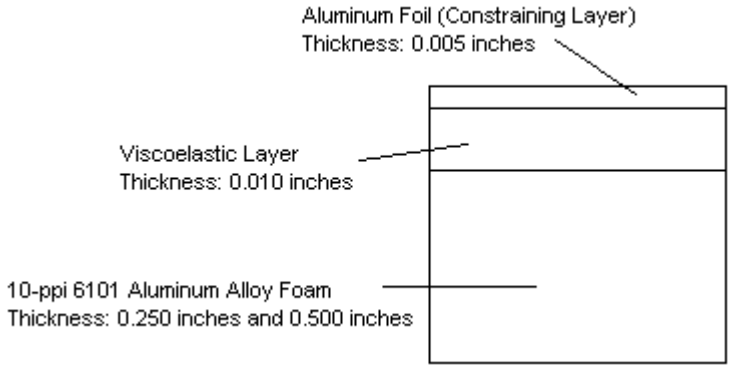


Figure 6. The constrained viscoelastic layer schematic

The viscoelastic layer was applied over the surface of the aluminum foam. The viscoelastic material was made by 3M and is primarily made of silicone. The nominal thickness of the viscoelastic layer is 0.010 inches at a nominal temperature between 20 to 90 degrees Celsius. The constraining layer applied above the viscoelastic layer was aluminum foil with a nominal thickness of 0.005 inches. The viscoelastic layer uses the

shear force to absorb and dissipate energy of the aluminum foam [Ref. 6]. Figure 7 was the aluminum foam using a constrained viscoelastic layer to increase damping

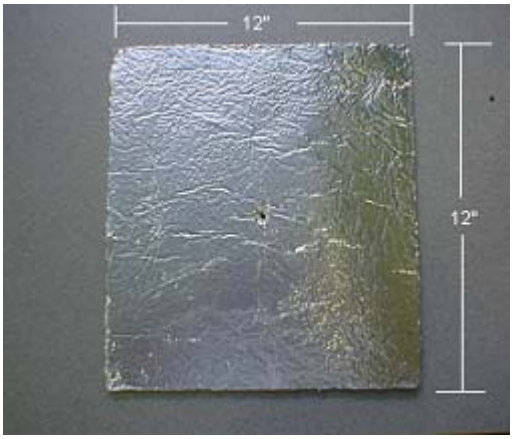


Figure 7. The aluminum foam with a constrained viscoelastic layer

The aluminum foam, the viscoelastic-aluminum foam composite, aluminum foam with a constrained viscoelastic layer, and the solid pieces of aluminum had the following weights.

| Materials | Weight (lbs) |
|---|---|
| 1/8” thick Solid Aluminum | 1.30 |
| 1/4" Thick Solid Aluminum | 2.61 |
| 1/2" Thick Aluminum Foam | 0.48 |
| 1/4" Thick Aluminum Foam | 0.24 |
| Composite | 1.36 |

| 1/4" Thick Aluminum Foam | 1 Side (lbs) | 2 Sides (lbs) |
|---|---|---|
| 1 Layer | 0.38 | 0.51 |
| 2 Layers | 0.52 | 0.78 |
| 3 Layers | 0.65 | 1.05 |
| 1/2" Thick Aluminum Foam | | |
| 1 Layer | 0.61 | 0.75 |
| 2 Layers | 0.75 | 1.02 |
| 3 Layers | 0.89 | 1.28 |

Table 1. Weights of the materials

The base material weights are located on the left table. The weights of the constrained viscoelastic layer can be found on the right table. The right table summarizes the weights of the 10-ppi quarter-inch 6101 aluminum alloy with 1, 2 and 3 constrained viscoelastic layers applied to one side and both sides. Also listed in the right table are the weights of the 10-ppi half-inch 6101 aluminum alloy with 1, 2 and 3 constrained viscoelastic layers applied to one side and both sides.

THIS PAGE INTENTIONALLY LEFT BLANK

# II. THEORY

## A. FORCED VIBRATION

Determining the frequency response is the bases for accurately determining the damping ratios and natural frequencies of a material.

The following equation is the equation of motion for a single degree-of-freedom system (1-DOF).

$$m\ddot{x} + c\dot{x} + kx = F(x) \tag{2.1}$$

$m$ = Mass of the system
$c$ = Damping of the system
$k$ = Stiffness of the system
$x$ = Displacement of the system
$\dot{x}$ = Velocity of the system
$\ddot{x}$ = Acceleration of the system
$F(x)$ = Force applied to the system

To solve the differential equation, a solution for the displacement is assumed. Also the force applied to the aluminum foam during the experiment was harmonic. Equation 2.2 is the solution for the displacement and equation 2.3 is the harmonic force applied to the mass.

$$x = Xe^{i\omega t} \tag{2.2}$$

$$F(x) = Fe^{i\omega t} \tag{2.3}$$

$\omega$ = Frequency of applied force
$t$ = Time

By differentiating equation 2.2 to determine the velocity and acceleration the displacement magnitude can be determined from the equation of motion. Equation 2.1 becomes the following equation after the equations for the displacement, velocity, and acceleration have been substituted into the equation of motion.

$$H(\omega) = \frac{X(\omega)}{F(\omega)/k} = \frac{k}{k - m\omega^2 + ci} \tag{2.4}$$

H is the frequency response of the system. By factoring the stiffness from the denominator and substituting the following equations into equation 2.4,

$$\omega_n^2 = \frac{k}{m} \qquad \zeta = \frac{c}{c_c} = \frac{c}{2\sqrt{km}} \tag{2.5}$$

$\omega_n$ = Natural frequency

$\zeta$ = Damping ratio

$c_c$ = Critical damping coefficient

the frequency response can be written in the classical form:

$$H(\omega) = \frac{1}{1 - \left(\frac{\omega}{\omega_n}\right)^2 + 2\zeta\left(\frac{\omega}{\omega_n}\right)i} \tag{2.6}$$

For a 1-DOF system, there is one natural frequency and one damping ratio. For multiple degrees-of-freedom (multi-DOF), there are as many natural frequencies and damping ratios as there are DOF. Modal analysis can be used to analyze a multi-DOF system. The following equation is the general form for a multi-DOF system:

$$[m]\{\ddot{x}\} + [c]\{\dot{x}\} + [k]\{x\} = \{F\} \tag{2.7}$$

The mass, damping, and stiffness matrixes are n by n in size, with n being the number of DOF in the system. The force, displacement, velocity and acceleration vectors are n by 1 in size. Each element in the vectors corresponds to a DOF of the system. The mass and stiffness matrixes are symmetric and may have some form of coupling. The first step to analyze the multi-DOF system is to determine the natural frequencies and mode shapes by analyzing the free response of the system. The general form of the free response of motion for a multi-DOF system is as follows:

$$[m]\{\ddot{x}\} + [k]\{x\} = 0 \tag{2.8}$$

Using equation 2.2 for each of the DOF, equation 2.7 will reduce to the following equation:

$$\left[k_{ij} - m_{ij}\omega^2\right]\{x\} = 0 \quad i = 1...n \qquad j = 1...n \tag{2.9}$$

The indexes i and j correspond to the element locations in the mass and stiffness matrixes. From the above equation, a solution for the displacements can be $\{x\} = 0$ if the matrix, $\left[k_{ij} - m_{ij}\omega^2\right]$, is invertible. This solution, however, is the trivial solution. To ensure the matrix is not invertible, the determinant of the matrix is forced to equal zero. This is accomplished by finding the values of frequency that would set the matrix determinant equal to zero. By forcing the matrix determinant equal to zero, the matrix will now be singular and an inverse does not exist, and therefore a non-trivial solution can be found. The frequencies determined in this way are the eigenvalues of the matrix and are the natural frequencies. Also the eigenvectors of the matrix are the mode shapes of the system. The mode shapes of a system illustrates how the system responses to an excitation at the corresponding natural frequency. The first mode shape is associated with the lowest natural frequency; the second mode shape corresponds to the next lowest frequency and so on. The modal matrix is formed by placing the mode shape vectors as the columns of the matrix.

$$[\Phi] = \left[\{\phi\}^1 \{\phi\}^2 ... \{\phi\}^n\right] \tag{2.10}$$

$\Phi$ is the modal matrix and $\phi$ are the mode shape vectors. The modal matrix will have the same number of rows and columns as there are DOF's. All the modes of a vibration system are orthogonal.

To decouple equation 2.7, we assume a set of modal coordinates.

$$\{x\} = [\Phi]\{q\} \quad \{\dot{x}\} = [\Phi]\{\dot{q}\} \quad \{\ddot{x}\} = [\Phi]\{\ddot{q}\} \tag{2.11}$$

The next step is to substitute the above equations into equation 2.7 and multiply both sides by the transpose of the modal matrix.

$$[\Phi]^T [m][\Phi]\{\ddot{q}\} + [\Phi]^T [c][\Phi]\{\dot{q}\} + [\Phi]^T [k][\Phi]\{q\} = [\Phi]^T \{F\} \tag{2.12}$$

Using the orthogonal properties of the modal matrix and the symmetric properties of the mass, damping and stiffness matrix results in the following equation.

$$[\tilde{m}_{ii}]\{\ddot{q}\}+[\tilde{c}_{ii}]\{\dot{q}\}+[\tilde{k}_{ii}]\{q\}=[\Phi]^T\{F\} \tag{2.13}$$

The new modal mass, damping, and stiffness matrixes are diagonal. As a result, the modal coordinates are decoupled and can be solved for each DOF in the same manner as equation 2.1. Equation 2.13 can be further simplified by multiplying both sides by the inverse of the modal mass matrix [Ref. 7].

$$\{\ddot{q}\}+[2\zeta_{ii}\omega_{ii}]\{\dot{q}\}+[\omega_{ii}^2]\{q\}=\{\tilde{F}\} \qquad \{\tilde{F}\}=[\tilde{m}]^{-1}[\Phi]^T\{F\} \tag{2.14}$$

## B. HALF-POWER POINT METHOD

The damping ratio for equation 2.14 was calculated experimentally by using the half-power point method. The half-power point method determines the damping ratio by examining the sharpness of the resonance peak. The following equation is the magnitude of the frequency response

$$H=\frac{1}{\sqrt{\left[1-\left(\frac{\omega}{\omega_n}\right)^2\right]^2+\left[2\zeta\left(\frac{\omega}{\omega_n}\right)\right]^2}} \tag{2.15}$$

At resonance, the magnitude of the frequency response is $H_{resonance}=1/2\zeta$. The next step is to square both sides of equation 2.16 and determine the frequencies that correspond to one-half the $H_{resonance}$.

$$\frac{1}{2}\left(\frac{1}{2\zeta}\right)=\frac{1}{\left[1-\left(\frac{\omega}{\omega_n}\right)^2\right]^2+\left[2\zeta\left(\frac{\omega}{\omega_n}\right)\right]^2}$$

or

$$\left(\frac{\omega}{\omega_n}\right)^4-2\left(1-2\zeta^2\right)\left(\frac{\omega}{\omega_n}\right)^2+\left(1-8\zeta^2\right)=0 \tag{2.16}$$

Solving for $(\omega/\omega_n)^2$ results in the following equation.

$$\left(\frac{\omega}{\omega_n}\right)^2 = \left(1-2\zeta^2\right) \pm 2\zeta\sqrt{1-\zeta^2} \tag{2.17}$$

Assuming that $\zeta << 1$, the higher order terms can be neglected. This results in the following equation.

$$\left(\frac{\omega}{\omega_n}\right)^2 = 1 \pm 2\zeta \tag{2.18}$$

Letting $\omega_1$ and $\omega_2$ correspond to each of the frequencies above and $\omega_2 > \omega_1$, the difference of $\omega_2$ and $\omega_1$ is illustrated in the following equation.

$$4\zeta = \frac{\omega_2^2 - \omega_1^2}{\omega_n^2} \cong 2\left(\frac{\omega_2 - \omega_1}{\omega_n}\right) \tag{2.19}$$

The damping ratio can now be determined by rearranging equation 2.19 [Ref. 7]

$$\zeta = \frac{\omega_2 - \omega_1}{2\omega_n} = \frac{f_2 - f_1}{2f_n} \tag{2.20}$$

THIS PAGE INTENTIONALLY LEFT BLANK

# III. EXPERIMENTAL SETUP

## A. EQUIPMENT DESCRIPTION

The equipment used during the experiment were as follows:

- Hewlett Packard 3562A Dynamic Signal Analyzer
- Wilcoxon Research Model F4 Electromagnetic Shaker
- Wilcoxon Research Model Z7 Transducer Base
- Wilcoxon Research Model PA7C Power Amplifier
- Wilcoxon Research Model N7C Matching Network
- Piezotronics Modally Tuned Impact Hammer
- Piezotronics Accelerometer

The Hewlett Packard 3562A dynamic signal analyzer was used to compute the frequency response of the aluminum foam. The HP 3562A Dynamic Signal Analyzer is a dual-channel, fast Fourier transform-based network, spectrum and waveform analyzer that provides analysis capabilities in both the time and frequency domains. Two input channels and a built-in signal source (noise and sine signals) can be used to perform the spectrum analysis. The signal analyzer has a frequency resolution of 25.6 μHz allowing the user to obtain highly accurate, high-resolution plots of the frequency responses of the mechanical system. Single channel accuracy is ± 0.15 dB with 80 dB of dynamic range. For transient or waveform analysis, signals can be sampled, digitized then stored in an internal memory, or directed via HP-IB to an external computer. The stored waveforms can be recalled and analyzed in the time and frequency domains using MATLAB or any other number manipulating software [Ref. 10].

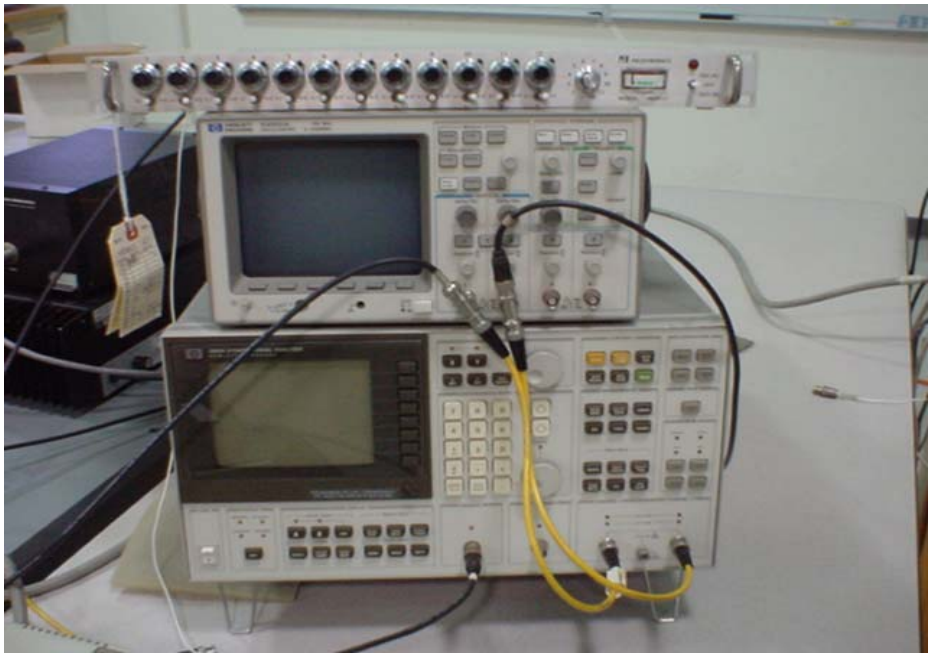

Figure 8. The Hewlett Packard 3562A dynamic signal analyzer and oscilloscope

The Wilcoxon Research Model F4 Electromagnetic Shaker is a ring shaped permanent magnet shaker. Its light coil and bobbin are rigidly attached to the transducer base that the F4 encircles. Two rubber diaphragms suspend the heavier magnets, one near the top and the other near the base of the transducer base just above the force gage. The F4 shaker is powered from the PA7C Power Amplifier. The shaker can be air-cooled to allow operations above normal operating currents. The specimen is attached to the shaker by means of a threaded stud. The contacting surface of the test specimen and contact surface of the mounting base must be inspected for grit and burrs prior to attachment to insure the accuracy of the transducer sensitivity [Ref. 11].

Figure 9. The Wilcoxon Research Model F4 Electromagnetic Shaker

The Wilcoxon Research Model Z7 Transducer Base consists of a cylindrical titanium housing containing Piezotronics accelerometer and a Piezotronics force gage. The accelerometer has a sensitivity of 10 mV / g and the force gage 10 mV / lbf [Ref. 11].

The Wilcoxon Research Model PA7C Power Amplifier has two independently operated amplifier channels to operate the shaker system. Each channel has a separate amplification control driven by a common oscillator input. The amplifier's 115 watts per channel (250 watts in mono mode) power rating is sufficient for many small shaker requirements [Ref. 11].

The Wilcoxon Research Model N7C Matching Network provides impedance matching for the reactive load of the F7 shaker and overload protection for the F4 shaker. The power cord is located in the rear of the N&C and plugs directly into the PA7C Power Amplifier. The output connections to the F4 shaker are located on the front panel. A front panel toggle switch selects circuit breakers to provide overheating protection. The air-cooled position is used when the F4 is being cooled with forced air but also may be used for a short duration operation at higher amperage drive levels without air-cooling [Ref. 11].

The Piezotronics Modally Tuned Impact Hammer was the series 086B03 SN2194 model. The modally tuned hammer was capable to excite all structural resonances up to 10 kHz. The hammer would convert a transfer force into an electrical signal that was used by the Hewlett Packard 3562A Dynamic Signal Analyzer as the input response. The hammer has a sensitivity of 10 mV / lbf, weighs 0.3 lb, and has a total length of 8 inches.

Figure 10. The Piezotronics Modally Tuned Impact Hammer

The Piezotronics Accelerometer is a hermetically sealed, shear-structured ICP accelerometer. The accelerometer provides a 10 mV/g output over a frequency range from 1 to 20,000 Hz (±10%). The accelerometer has a total weight of 0.7 grams, therefore the inertial effects due to the weight of the transducer are considered negligible.

## B. EQUIPMENT SETUP

The equipment used a different setup for the swept sine, impact hammer, and random noise tests

### 1. Swept Sine

The swept sine test consisted of varying the input forcing frequency gradually in a specified frequency span. The input force was applied to the material by a 2-volt source from the Hewlett Packard 3562A Dynamic Signal Analyzer using the Wilcoxon Research Model F4 Electromagnetic Shaker. The signal analyzer was set in the swept sine mode. A stable mean of the output response was taken for 20 averages. The window selection was not needed for the swept sine mode. The output signal was determined in two ways. The

first way was to use the force gage located in the shaker as the input and the accelerometer located in the shaker as the output. The second way was to use the accelerometer in the shaker as the input and an external transducer located at a random point as the output. The test was used to determine the frequency response of the 10-ppi quarter-inch 6101 aluminum alloy foam, the viscoelastic-aluminum foam alloy, and the 10-ppi quarter-inch aluminum alloy foam using a constrained viscoelastic layer. Figure 11 and 12 are schematics of the equipment setup used to determine the frequency response of the material using the swept sine test.

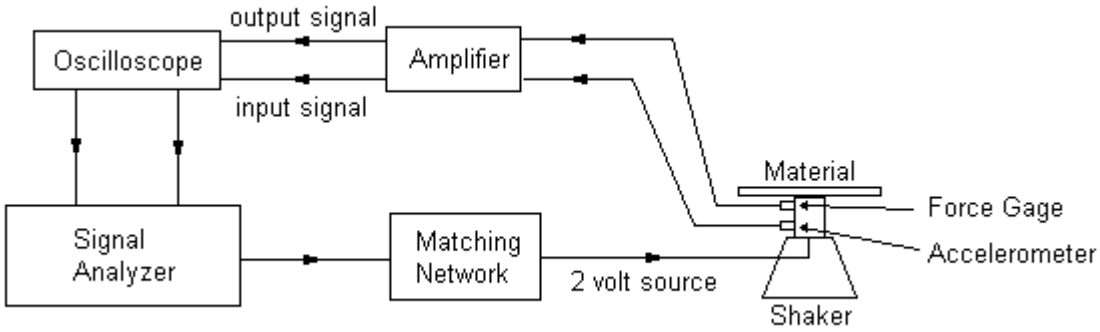


Figure 11. Equipment setup using the Wilcoxon Research Model F4 Electromagnetic Shaker. Input signal: force gage, Output signal: accelerometer

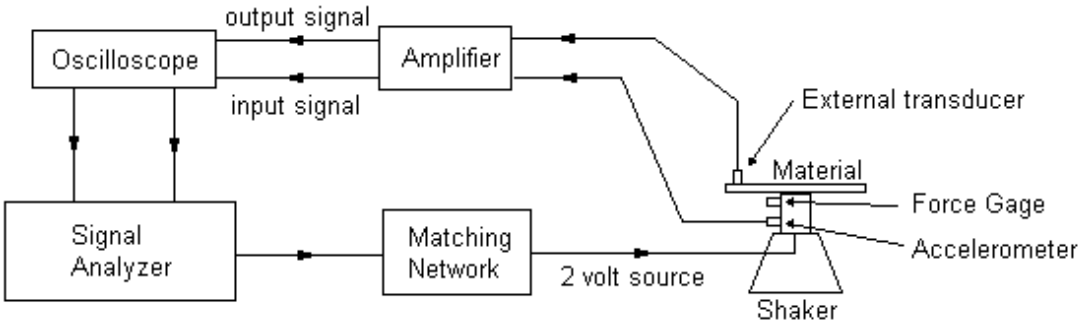


Figure 12. Equipment setup using the Wilcoxon Research Model F4 Electromagnetic Shaker. Input signal: accelerometer, Output signal: external transducer

## 2. Impact Hammer

The impact hammer test uses a modal hammer to excite modes of vibration within a material. The impact hammer test was used to determine the frequency response for the 10-ppi quarter-inch 6101 aluminum alloy foam and the viscoelastic-aluminum foam composite. The impact hammer test was used to examine the frequency modes from 0 to 250 Hz. A rubber tip was used for the hammer because a soft tip will produce a lower peak impact with a long force impact time. This is more suited for lower frequency responses. A harder tip was not used because the impact force would result in a larger peak force with a short force time, which is more suited for high frequency responses. The hammer was connected to the input channel of the signal analyzer and the external transducer was connected to the output channel of the signal analyzer. The material to be tested was supported by fishing line tied to a wooden apparatus.

Figure 13. Wooden apparatus support for the impact hammer test

The signal analyzer was set in the linear resolution mode. The force-exponential window was used during the impact hammer test. 20 stable mean averages were used to obtain the correct frequency response. The time record was set to trigger when the input signal from the hammer reached 0.5 volts. The equipment setup used for the test can be found in figure 14.

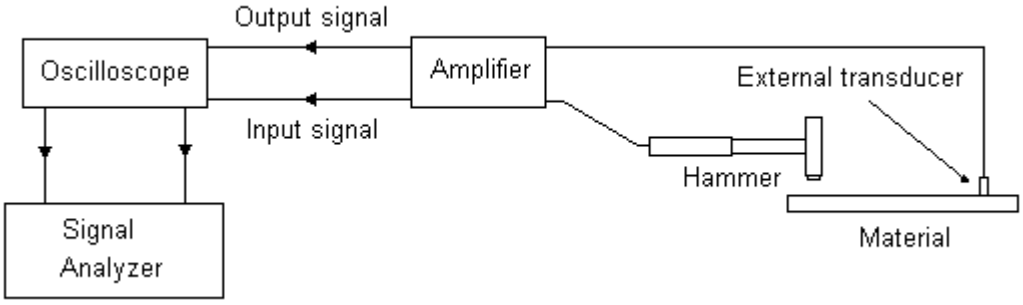


Figure 14. Equipment setup using the Piezotronics Modally Tuned Impact Hammer. Input signal: impact hammer, Output signal: external transducer

### 3. Random Noise

The random noise test inputs a signal that contains all the frequencies within a specified frequency span. The input signal was determined using the force gage located in the shaker and the output signal was determined using the accelerometer located in the shaker. The random noise test was used for the eighth-inch and quarter-inch aluminum plate and the 10-ppi quarter-inch and half-inch 6101 aluminum alloy foam with constrained viscoelastic layers. The equipment setup for the random test was the same as figure 11, but the dynamic signal analyzer setup differed from the swept sine configuration. The signal analyzer was set in the linear resolution mode. The window used for the experiment was a Hann window. A stable mean of the frequency response was determined using 50 averages. The source was set for a level of 2 volts in the random noise mode. The tests were conducted for a frequency span from 0 to 1000 Hz.

THIS PAGE INTENTIONALLY LEFT BLANK

# IV. RESULTS AND DISCUSSION

The tests used to determine the frequency response of the different materials were the swept sine test, impact hammer test, and the random noise test. The natural frequencies were determined from the frequency response. Once the natural frequencies were determined from the Nyquist and phase plots of the frequency response, a zoom measurement of the resonance peak was taken using a frequency span wide enough to accurately determine the damping ratio using the half-power point method.

## A. SWEPT SINE TESTS

The swept sine test was used to determine the frequency response for the 10-ppi quarter-inch 6101 aluminum alloy foam, the viscoelastic-aluminum foam composite, and the 10-ppi quarter-inch 6101 aluminum alloy foam using the constrained viscoelastic layer.

### 1. 10-ppi Quarter-Inch Aluminum Alloy Foam

For the 10-ppi quarter-inch 6101 aluminum alloy foam, the input was determined using the force gage located in the shaker and the output was determined using the accelerometer located in the shaker. The test was conducted for a frequency span from 0 to 250 Hz. Figure 15 is a sample frequency plot of the 10-ppi quarter-inch 6101 aluminum alloy foam determined using the swept sine test.

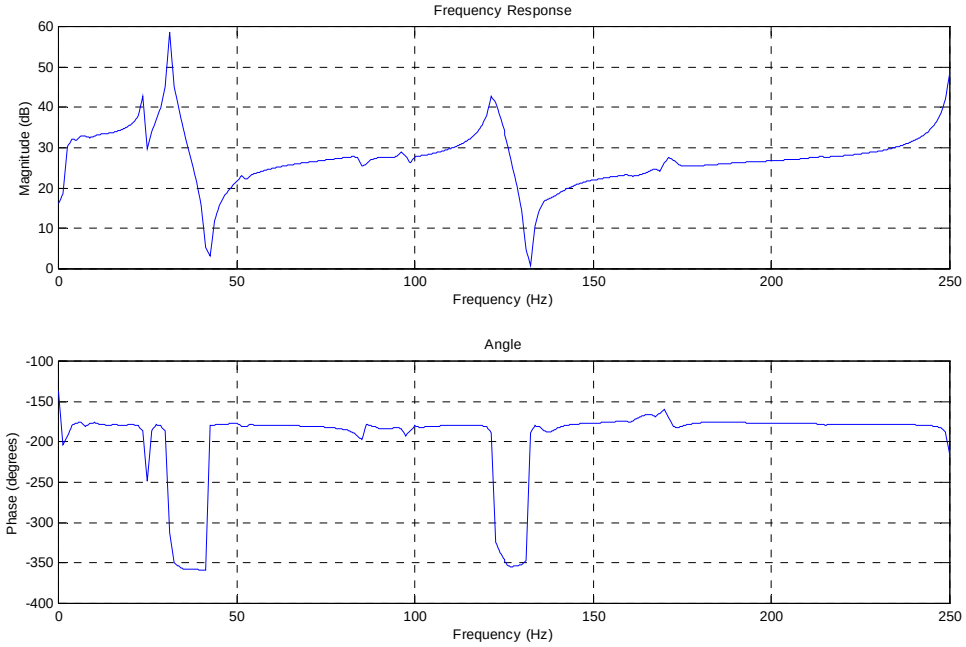


Figure 15. Frequency response and phase plot for the 10-ppi quarter-inch 6101 aluminum alloy foam. The input was the shaker force gage and the output was the shaker accelerometer

The locations of the natural frequencies for the 10-ppi quarter-inch 6101 were determined from frequency plots such as figure 15. The next step was to calculate the damping ratios by using a zoom measurement of the resonance peak by isolating the natural frequencies in a frequency band that would capture the correct characteristics of the peak. Figure 16 is an example of a resonance peak used to determine the damping ratios associated with each natural frequency.

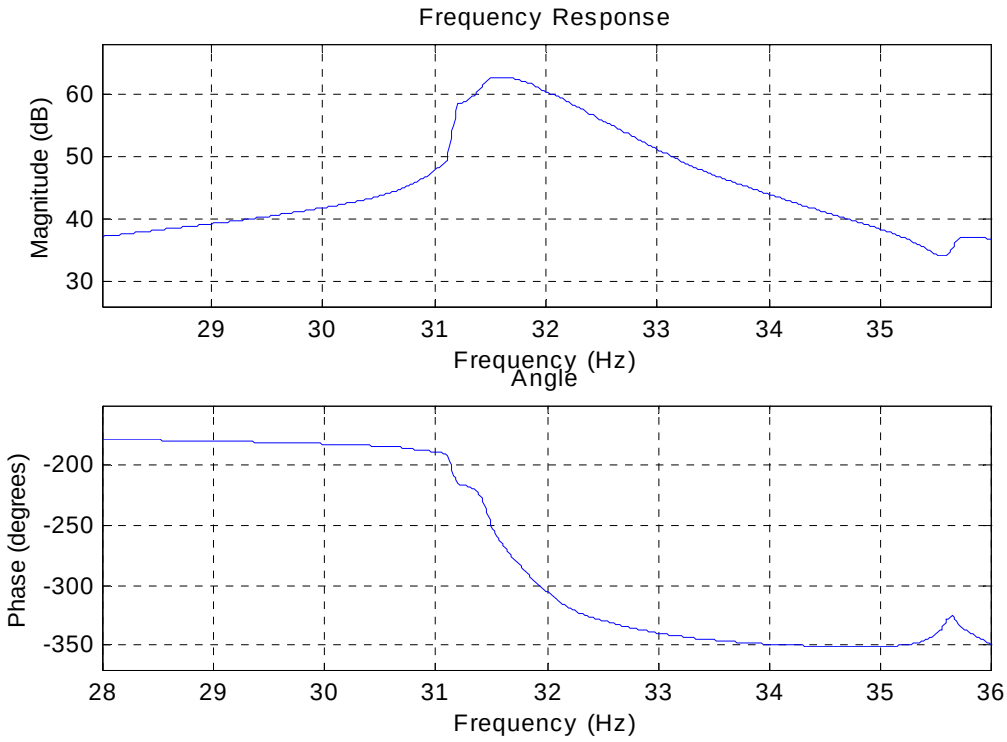


Figure 16. Sample phase and frequency plot for the 10-ppi quarter-inch 6101 aluminum alloy foam. The input was the shaker force gage and the output was the shaker accelerometer

Table 2 summarizes all the natural frequencies and damping ratios for the 10-ppi quarter-inch 6101 aluminum alloy foam using the shaker force gage as the input and the shaker accelerometer as the output signal. The frequency range used in the experiment was 0 to 250 Hz.

| $\omega_n$ (Hz) | $\zeta$ (%) |
|---|---|
| 22.90 | 1.31 |
| 29.00 | 1.03 |
| 50.80 | 0.20 |
| 115.90 | 0.32 |
| 228.88 | 0.13 |

Table 2. Natural frequencies and damping ratios for 10-ppi quarter-inch 6101 aluminum alloy foam determined by the swept sine test. Input: Force Gage, Output: Accelerometer

The next test was to calculate the damping ratio from a random point on the 10-ppi quarter-inch 6101 aluminum alloy foam. The accelerometer located in the shaker was used as the input. The external transducer was used to calculate the output response. The transducer was applied to the material using a piece of aluminum foil and wax. The aluminum foil was necessary to provide a consistent flat surface for the transducer. The more layers of aluminum foil applied to the surface resulted in a smoother surface, but the effect of the aluminum foil on the frequency response was unknown. To determine the effect of the aluminum foil, the natural frequencies and damping ratios were calculated using the accelerometer in the shaker as the input and the output determined at the random point x using 1, 2, and 3 layers of aluminum foil for the transducer. The random point locations can be found in figure 17.

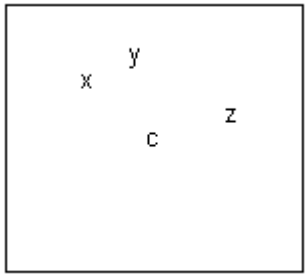


Figure 17. Random point x, y, and z locations for the external transducer

The random points remained the same for all tests conducted in the experiment to maintain consistency within the results. The results of the number of foil layers tests are summarized in table 3.

| 1 foil | | 2 foil | | 3 foil | |
|---|---|---|---|---|---|
| $\omega_n$ (Hz) | $\zeta$ (%) | $\omega_n$ (Hz) | $\zeta$ (%) | $\omega_n$ (Hz) | $\zeta$ (%) |
| 22.85 | 1.48 | 22.48 | 1.56 | 22.78 | 1.81 |
| 29.10 | 0.73 | 29.10 | 0.82 | 29.12 | 0.73 |
| 33.70 | 0.41 | 33.63 | 0.22 | 33.57 | 0.30 |
| 50.95 | 0.41 | 50.75 | ------ | 51.10 | 0.26 |
| 115.90 | 0.33 | 115.90 | 0.30 | 115.65 | 0.26 |
| 160.25 | 0.21 | 160.23 | 0.26 | 160.10 | 0.21 |
| 162.68 | ------ | 163.65 | ------ | 162.25 | ------ |
| 167.50 | 0.46 | 167.50 | 0.25 | 167.30 | 0.44 |
| 183.40 | 0.19 | 183.2 | 0.27 | 183.00 | 0.36 |
| 228.35 | 0.19 | 228.20 | 0.19 | 227.95 | 0.18 |

Table 3. Natural frequencies and damping ratios for at a random point for 10-ppi quarter-inch 6101 aluminum alloy foam with 1, 2, and 3 layers of aluminum foil for the output accelerometer.

Figure 18 is a plot of the information provided in table 3.

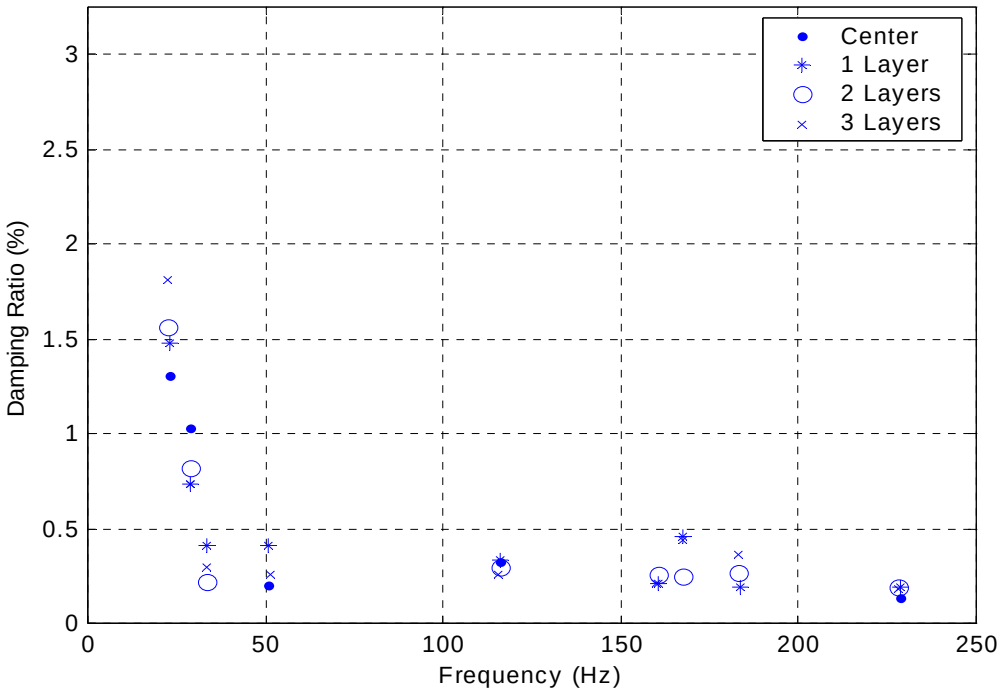


Figure 18. Comparison of the damping ratios and natural frequencies for the 10-ppi quarter-inch 6101 aluminum alloy foam with different foil layers using the swept sine test

The natural frequency varied only slightly, with the greatest difference for the natural frequencies being 1.40 Hz. The damping ratio had a maximum variation of 0.33%. The number of aluminum foil layers used had little effect on the output response, therefore one layer was used to provide the base for the output transmitter.

The next test was to determine the natural frequencies and damping ratios for random points y and z for the 10-ppi quarter-inch 6101 aluminum alloy foam. The following table is a comparison of the damping ratios and natural frequencies for all the output positions for the 10-ppi quarter-inch 6101 aluminum alloy foam using the swept sine test.

| **Center** | | **Point x** | | **Point y** | | **Point z** | |
|---|---|---|---|---|---|---|---|
| **$\omega_n$ (Hz)** | **$\zeta$ (%)** | **$\omega_n$ (Hz)** | **$\zeta$ (%)** | **$\omega_n$ (Hz)** | **$\zeta$ (%)** | **$\omega_n$ (Hz)** | **$\zeta$ (%)** |
| 22.90 | 1.31 | 22.85 | 1.48 | 22.70 | 1.29 | 22.65 | 1.02 |
| 29.00 | 1.03 | 29.10 | 0.73 | 29.10 | 0.69 | 29.15 | 0.81 |
| ------ | ------ | 33.70 | 0.41 | 33.60 | 0.28 | 33.50 | 0.60 |
| 50.80 | 0.20 | 50.95 | 0.41 | 50.70 | 0.34 | 50.65 | 0.44 |
| 115.90 | 0.32 | 115.90 | 0.33 | 115.50 | 0.28 | 115.55 | 0.32 |
| ------- | ------ | 160.25 | 0.21 | 159.90 | 0.22 | 160.4 | ------ |
| ------- | ------ | 162.68 | ------ | 162.85 | 0.44 | 162.45 | 0.48 |
| ------ | ------ | 167.50 | 0.46 | 167.70 | 0.29 | 167.14 | 0.28 |
| ------ | ------ | 183.40 | 0.19 | 183.60 | 0.39 | 183.50 | 0.36 |
| 228.88 | 0.13 | 228.35 | 0.19 | 229.00 | 0.18 | 228.25 | 0.20 |

Table 4. Summary of the natural frequencies and damping ratios determined for the 10-ppi quarter-inch 6101 aluminum alloy foam determined using the swept sine test

Figure 19 shows the locations of the natural frequencies and damping ratios determined for the 10-ppi quarter-inch 6101 aluminum alloy foam during the swept sine test.

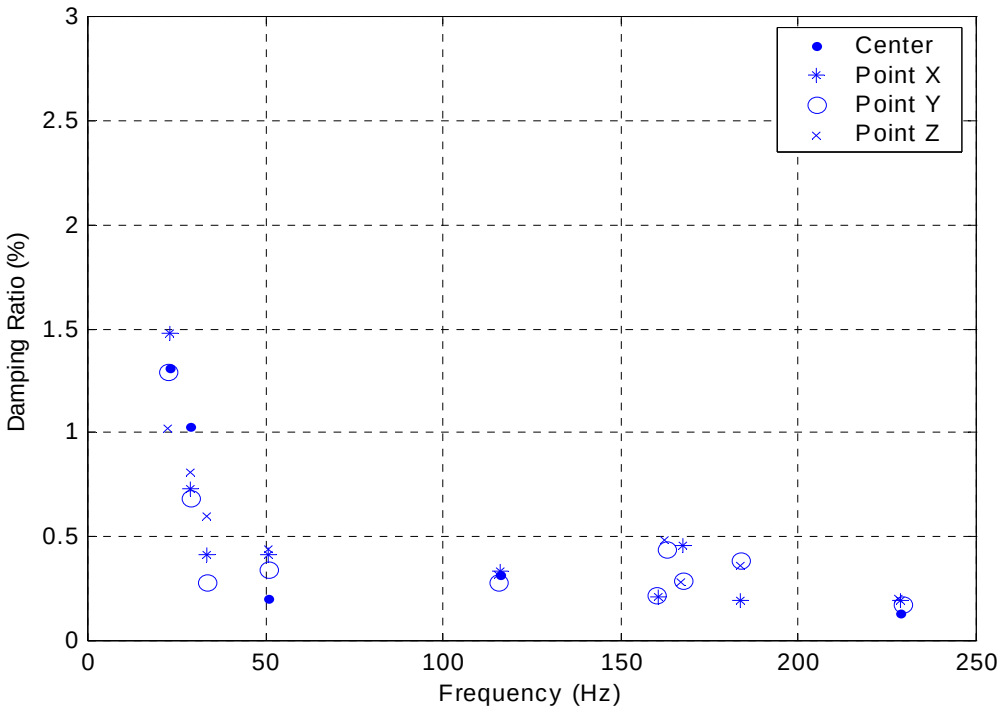


Figure 19. Comparison of the damping ratios and natural frequencies for the 10 ppi quarter-inch 6101 aluminum alloy foam using the swept sine test

In some cases, the natural frequencies was not determined for one point and was for another. This is because at some output positions, the output accelerometer was located at a node for a certain mode; therefore the natural frequency and damping ratio were not detectable at certain locations.

To compare the results of each test performed during the thesis, the average natural frequencies and damping ratios were calculated. The following table summarizes the average natural frequencies and damping ratios for the 10-ppi quarter-inch 6101 aluminum alloy foam determined by the swept sine test.

| $\omega_n$ (Hz) | $\zeta$ (%) |
|---|---|
| 22.78 | 1.28 |
| 29.09 | 0.82 |
| 33.60 | 0.43 |
| 50.78 | 0.35 |
| 115.71 | 0.31 |
| 160.18 | 0.22 |
| 162.66 | 0.46 |
| 167.45 | 0.34 |
| 183.50 | 0.31 |
| 228.62 | 0.18 |

Table 5. Average natural frequencies and damping ratios for the 10 ppi quarter-inch 6101 aluminum alloy foam using the swept sine test

### 2. Viscoelastic-Aluminum Foam Composite

The first swept sine test used for the viscoelastic-aluminum foam composite used the force gage as the input and the accelerometer as the output, both located in the shaker. The frequency response for the viscoelastic-aluminum foam composite indicated a fewer number of natural frequencies than the 10-ppi quarter-inch 6101 aluminum alloy foam for the frequency span from 0 to 250 Hz. Figure 20 is a sample frequency response for the composite material.

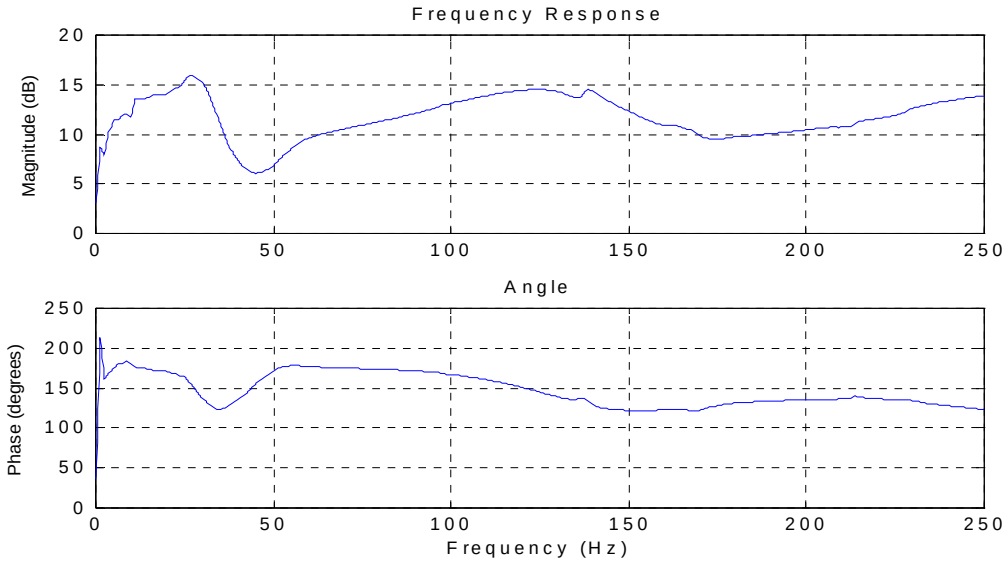


Figure 20. Sample frequency response for the viscoelastic-aluminum foam composite. The input was the shaker force gage and the output was the shaker accelerometer

As you can see from figure 20, the structure appears to exhibit higher damping characteristics than the viscoelastic-aluminum foam. Table 6 shows the natural frequencies and damping ratios determined for the viscoelastic-aluminum foam composite using the swept sine test for a frequency span from 0 to 250 Hz.

| Center | |
|---|---|
| $\omega_n$ (Hz) | $\zeta$ (%) |
| 24.34 | 26.32 |
| 106.82 | 28.18 |

Table 6. Natural frequencies and damping ratios for the viscoelastic-aluminum foam composite determined by the swept sine test for a frequency span from 0 to 250 Hz

The damping ratio increased dramatically through the viscoelastic treatment. The test was repeated using an accelerometer applied at points x, y, and z. The accelerometer did not have to be applied with aluminum foil because the composite surface could be sanded flat and attached with wax. Table 7 is a summary of the natural frequencies and damping ratios determined for the composite material using the swept sine mode for a frequency span of 0 to 250 Hz.

| Center | | Point x | | Point y | | Point z | |
|---|---|---|---|---|---|---|---|
| $\omega_n$ (Hz) | $\zeta$ (%) | $\omega_n$ (Hz) | $\zeta$ (%) | $\omega_n$ (Hz) | $\zeta$ (%) | $\omega_n$ (Hz) | $\zeta$ (%) |
| 24.34 | 26.32 | 27.55 | 28.23 | 28.21 | 27.13 | 28.00 | 26.43 |
| 121.82 | 28.18 | 126.82 | 29.40 | 124.15 | 29.40 | 123.27 | 28.73 |

Table 7. Natural frequencies and damping ratios for the viscoelastic-porous aluminum composite determined by the swept sine test. The input was the accelerometer located on the shaker and the output was the external transducer located at point x, point y, and point z.

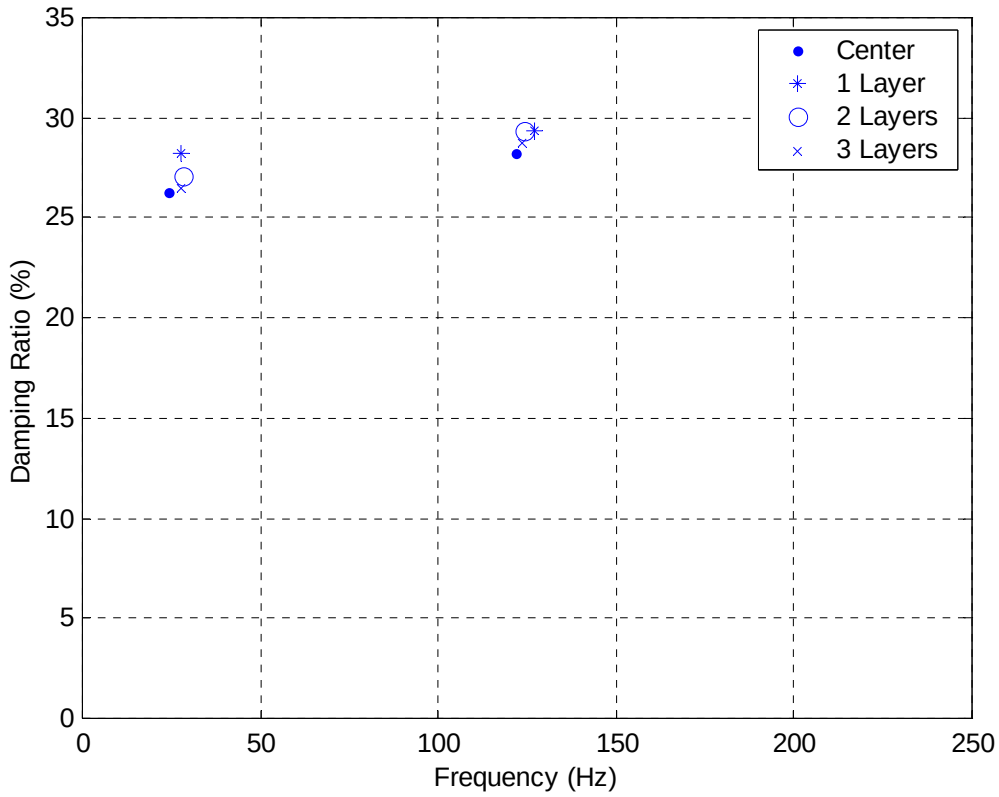


Figure 21. Comparison of the damping ratios and natural frequencies for the viscoelastic-aluminum foam composite using the swept sine test

As you can see from figure 21 the viscoelastic-aluminum foam composite damping treatment resulted in a large increase in the damping ratio. Unfortunately, the viscoelastic-aluminum foam composite is less stiff and is a much heavier material. The 10-ppi quarter-inch 6101 aluminum alloy foam does not bend nearly as much as the viscoelastic-aluminum foam composite. Also the weight of the 10-ppi quarter-inch 6101 aluminum alloy foam was 0.24 lbs while the viscoelastic-aluminum foam composite weighed 1.36 lbs; an increase of 548 %. Table 7 shows the average natural frequencies and damping ratios determined using the swept sine method.

| $\omega_n$ (Hz) | $\zeta$ (%) |
|---|---|
| 27.03 | 27.03 |
| 124.02 | 28.93 |

Table 8. Average natural frequencies and damping ratios for the viscoelastic-aluminum foam composite using the swept sine test

### 3. Constrained Viscoelastic Layer

To determine the effectiveness of the constrained viscoelastic layer, the 10-ppi quarter-inch 6101 aluminum alloy foam was analyzed with one, two, and three constrained viscoelastic layers applied to one and both surfaces. Figure 22 is a sample frequency response for the 10-ppi quarter-inch 6101 aluminum alloy foam with 2 constrained viscoelastic layers applied to both sides using the swept sine test for a frequency span from 0 to 250 Hz.

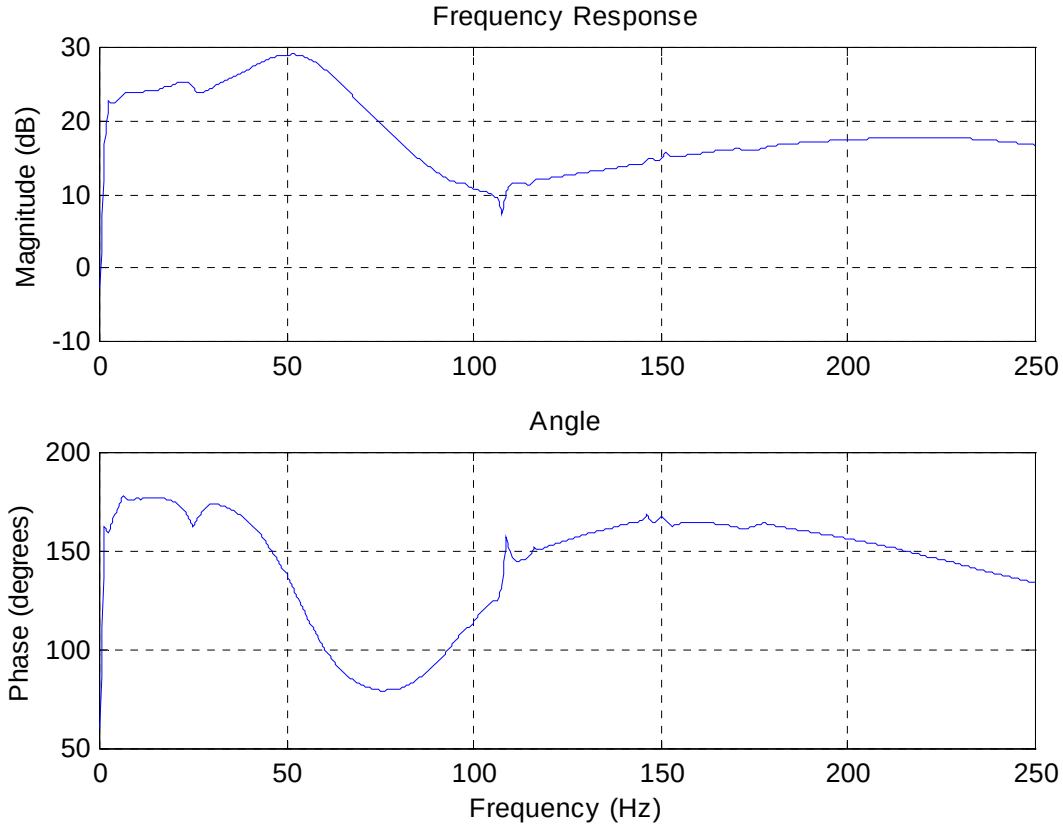


Figure 22. Sample Frequency Response for the 10-ppi quarter-inch 6101 aluminum alloy foam with two constrained viscoelastic layers applied to both sides of the aluminum foam. The input was the shaker force gage and the output was the shaker accelerometer

The test was conducted using the swept sine test using the same procedure as for the 10-ppi quarter-inch 6101 aluminum alloy foam and viscoelastic-aluminum foam composite. The natural frequencies and damping ratios determined in the experiment can be found in table 9.

| 1 Side | | | | | |
|---|---|---|---|---|---|
| $\omega_n$ (Hz) | $\zeta$ (%) | $\omega_n$ (Hz) | $\zeta$ (%) | $\omega_n$ (Hz) | $\zeta$ (%) |
| 40.00<br>165.81 | 8.70<br>13.45 | 42.00<br>167.25 | 9.52<br>18.13 | 42.88<br>172.81 | 14.61<br>18.58 |
| **2 Sides** | | | | | |
| $\omega_n$ (Hz) | $\zeta$ (%) | $\omega_n$ (Hz) | $\zeta$ (%) | $\omega_n$ (Hz) | $\zeta$ (%) |
| 53.15<br>241.03 | 19.80<br>22.15 | 63.24<br>------ | 26.59<br>------ | 60.63<br>------ | 29.13<br>------ |

Table 9. Summary of the damping ratios and natural frequencies for the 10 ppi quarter-inch 6101 aluminum alloy foam with 1, 2, and 3 constrained viscoelastic layers applied to one and both surfaces of the aluminum foam.

From table 9, as the number of constraining layers increases the damping ratio increases. Also, the constraining layers were more effective when applied to both sides of the 10-ppi quarter-inch 6101 aluminum alloy foam.

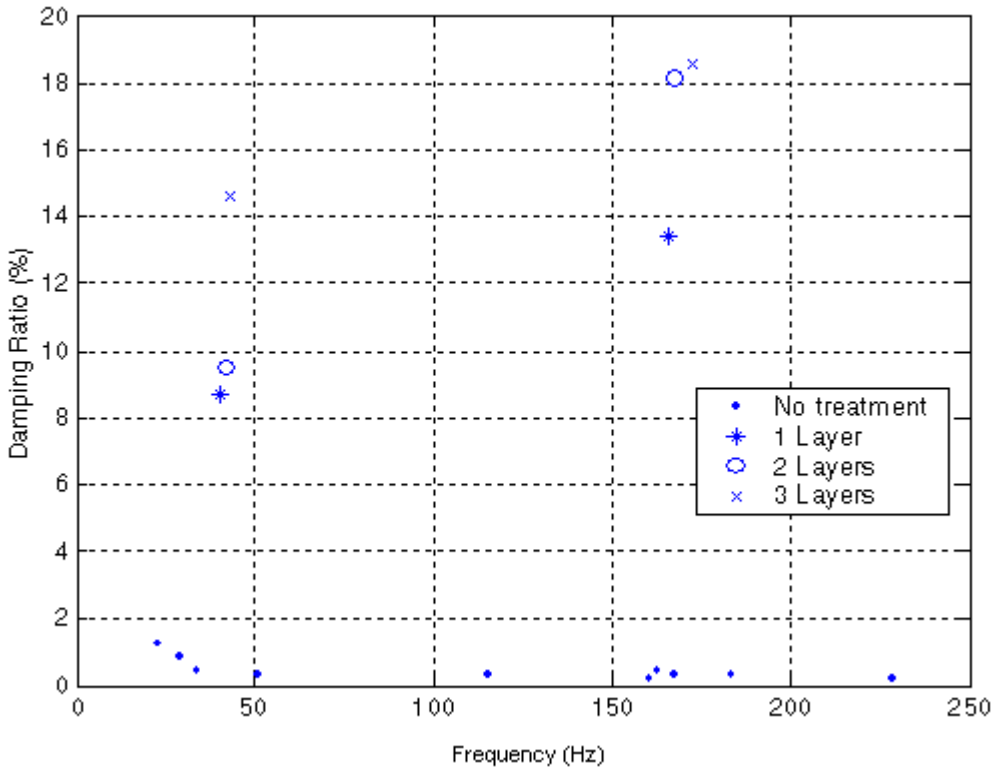


Figure 23. Natural frequencies and damping ratios for the 10 ppi quarter-inch 6101 aluminum alloy foam with 1, 2, and 3 constrained viscoelastic layers applied to one side of the aluminum foam

Figure 23 shows the damping ratio is increased to a maximum value of 18.58% when 3 constrained viscoelastic layers are applied to 1 side of the 10-ppi quarter-inch 6101 aluminum alloy foam, but the constrained viscoelastic layer was most effectiveness in increasing the damping ratio when the first constrained viscoelastic layer was applied to the 10-ppi quarter-inch 6101 aluminum alloy foam. Figure 24 shows the effectiveness of the constrained viscoelastic layers when applied to both sides of the 10-ppi quarter-inch 6101 aluminum alloy foam.

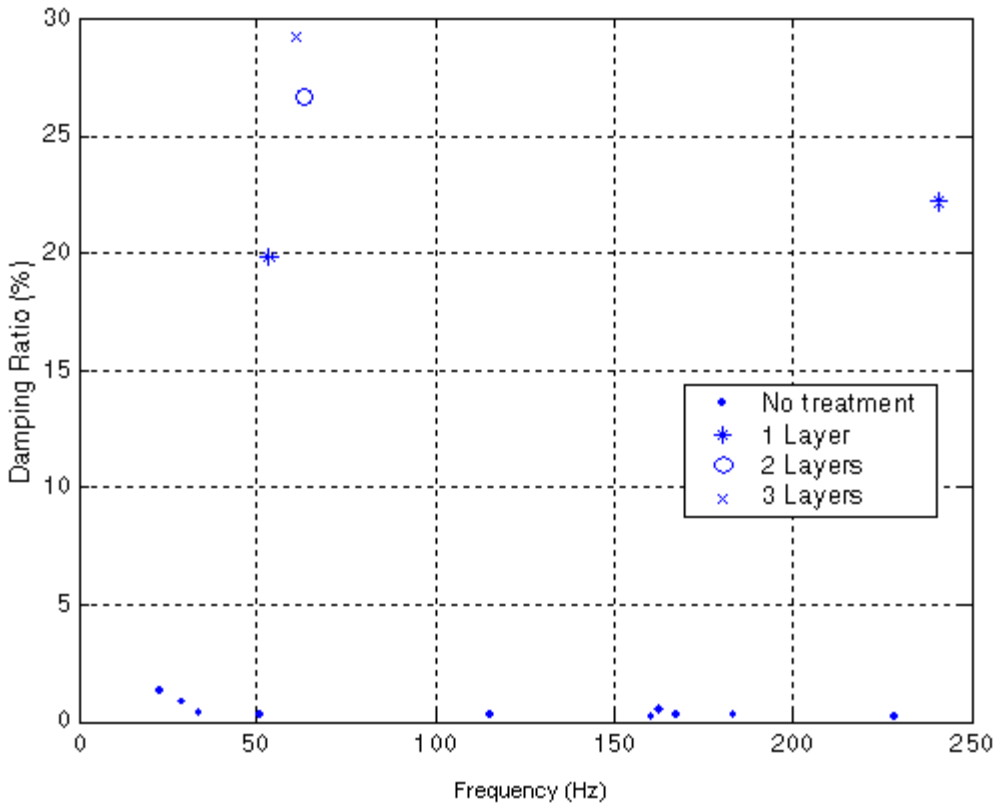


Figure 24. Natural frequencies and damping ratios for the 10 ppi quarter-inch 6101 aluminum alloy foam with 1, 2, and 3 constrained viscoelastic layers applied to both sides of the aluminum foam

As with the case for the constrained viscoelastic layer applied to one side of the 10 ppi quarter-inch 6101 aluminum alloy foam, the more constrained viscoelastic layers applied to the surface resulted in a higher damping ratio. The damping ratio reaches a peak of 29.13% for the 3 constrained viscoelastic layers case. Unfortunately the weight of the 10-ppi quarter-inch 6101 aluminum alloy foam also increased from 0.21 to 1.05 lbs. As with the constrained viscoelastic layer applied to one side of the aluminum foam, the

damping ratio change was greatest when the first constrained viscoelastic layer was applied to both sides of the aluminum foam. Each subsequent layer increased the damping ratio but not a large as the first layer. Also the weight increased to 0.51 lbs when one layer was applied to both sides of the aluminum foam. The one constrained viscoelastic layer applied to both sides of the aluminum foam did not increase the damping ratio as high as the viscoelastic-aluminum foam composite (maximum damping ratio for the viscoelastic-aluminum composite was 28.93% vice 22.15% for the one constrained viscoelastic layer applied to both sides of the aluminum foam), but the stiffness of the constrained viscoelastic layer applied to the aluminum foam was much higher than the stiffness for the viscoelastic-aluminum foam composite. Also the weight of the constrained viscoelastic layer applied to both sides of the aluminum foam was 1.67 times less than the viscoelastic-aluminum foam composite (1.36 lbs for the viscoelastic-aluminum foam composite and 0.51 lbs for the constrained viscoelastic layer applied to both sides of the aluminum foam).

## B. IMPACT HAMMER

The impact hammer was used to reinforce the data collected from the swept sine tests. The impact hammer was used for the 10-ppi quarter-inch 6101 aluminum alloy foam and the viscoelastic-aluminum foam composite.

### 1. 10-ppi Quarter-Inch 6101 Aluminum Alloy Foam

The 10-ppi quarter-inch 6101 aluminum alloy foam was suspended by fishing line by a wooden structure for the test. The first problem was establishing a striking point for the hammer. The surface of the 10-ppi quarter-inch 6101 aluminum alloy foam was inconsistent which made striking the material inconsistent. Also, both materials tended to slip or jump within the fishing line suspension. Even though the dynamic signal analyzer may have indicated a consistent force magnitude, the slipping and jumping of the material in the suspension would alter the frequency response and the accuracy of the test was lost. Despite the inaccuracies, the test was conducted with the hammer striking a random point while the accelerometer measured the output at another random point. The dynamic signal analyzer took the stable mean of 20 impacts for three cases. The three tests were conducted as follows:

- Striking point x and determining the response of the system with an external transducer at point y.
- Striking point x and determining the response of the system with an external transducer at point z.
- Striking point y and determining the response of the system with an external transducer at point z.

The results of the impact hammer tests for the 10-ppi quarter-inch 6101 aluminum alloy foam can be found in table 10.

| First test | | Second test | | Third test | |
|---|---|---|---|---|---|
| $\omega_n$ (Hz) | $\zeta$ (%) | $\omega_n$ (Hz) | $\zeta$ (%) | $\omega_n$ (Hz) | $\zeta$ (%) |
| 58.38 | 2.68 | 58.38 | 2.89 | 58.10 | 2.77 |
| 137.88 | 1.54 | 136.37 | 1.05 | 137.50 | 1.35 |
| ------ | ------ | 143.62 | 1.31 | ------ | ------ |
| 179.00 | 1.05 | 178.00 | 1.09 | 178.30 | 1.11 |
| 243.00 | ------ | 239.63 | 1.07 | 237.40 | 0.84 |

Table 10. Natural frequencies and damping ratios of the 10-ppi quarter-inch 6101 aluminum alloy foam using the impact hammer test

The damping ratios and natural frequencies vary from the values determined in the swept sine test. The damping ratios for the impact hammer test are higher than the values determined in the swept sine test. The maximum damping ratio determined for the 10-ppi quarter-inch 6101 aluminum alloy foam in the swept sine test was 1.28 % while the impact hammer test calculated a maximum damping ratio of 2.89 %.

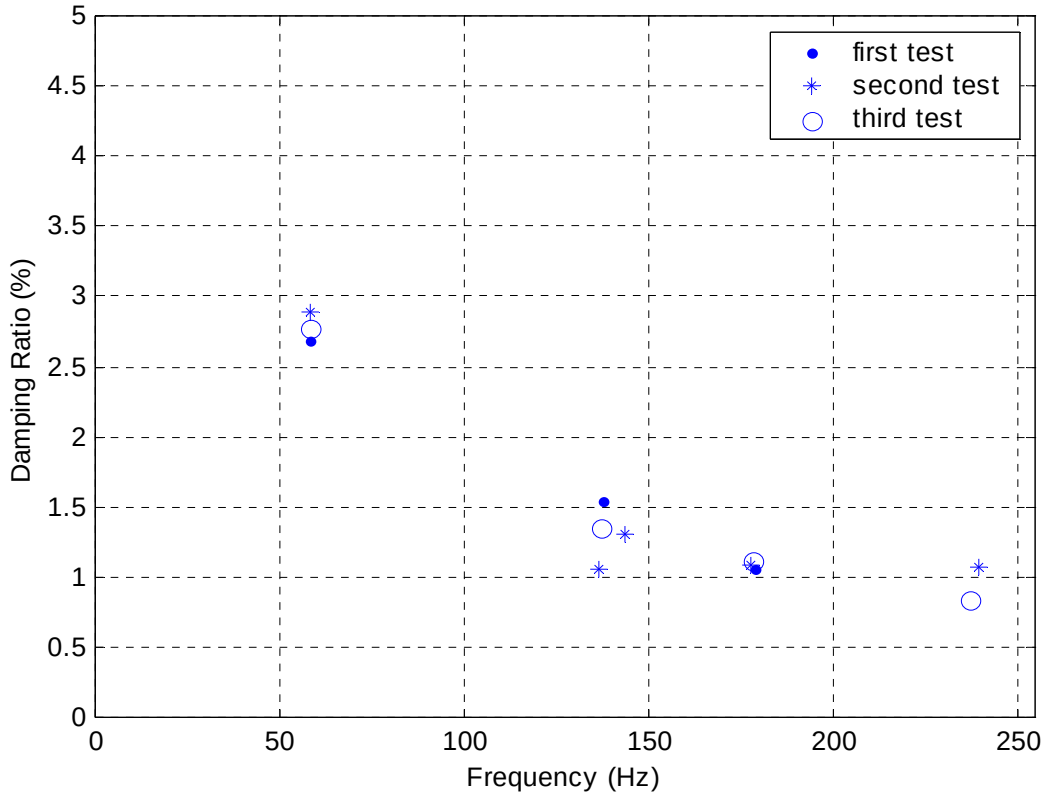


Figure 25. Comparison of the damping ratios and natural frequencies for the quarter inch porous aluminum using the impact hammer test

Figure 25 shows the values determined for the damping ratios and natural frequencies are consistent for each of the tests. Table 11 lists the average natural frequencies and damping ratios for the 10-ppi quarter-inch 6101 aluminum alloy foam determined using the impact hammer test.

| $\omega_n$ (Hz) | $\zeta$ (%) |
|---|---|
| 58.29 | 2.78 |
| 137.25 | 1.31 |
| 143.62 | 1.31 |
| 178.43 | 1.08 |
| 240.01 | 0.64 |

Table 11. Average natural frequencies and damping ratios for the 10-ppi quarter-inch 6101 aluminum alloy foam using the impact hammer test

### 2. Viscoelastic-Aluminum Foam Composite

The setup and test procedure for determining the damping ratios and natural frequencies for the viscoelastic-aluminum foam composite were the same as for the 10-ppi quarter-inch 6101 aluminum alloy foam. The natural frequencies were determined by examining the frequency response but less than half of the damping ratios were able to be determined using the half-power point method because the bandwidth at half power could not be determined. Figure 26 is sample of a frequency response of the composite material.

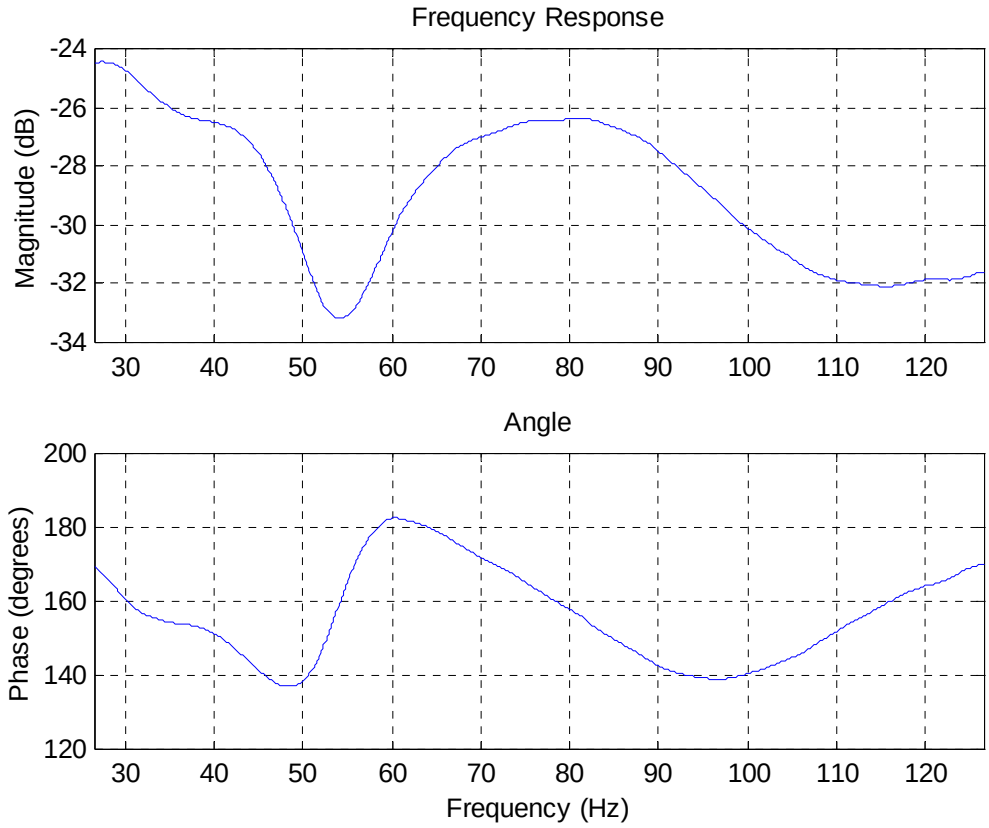


Figure 26. Sample frequency response for the viscoelastic-aluminum foam composite determined during the second test using the impact hammer test.

Figure 26 is a sample plot of a frequency response where the damping ratio could be determined because the half-power bandwidth for the resonance peak can be determined. Figure 27 is a sample plot of a frequency response where the damping ratio could not be determined using the half-power point method.

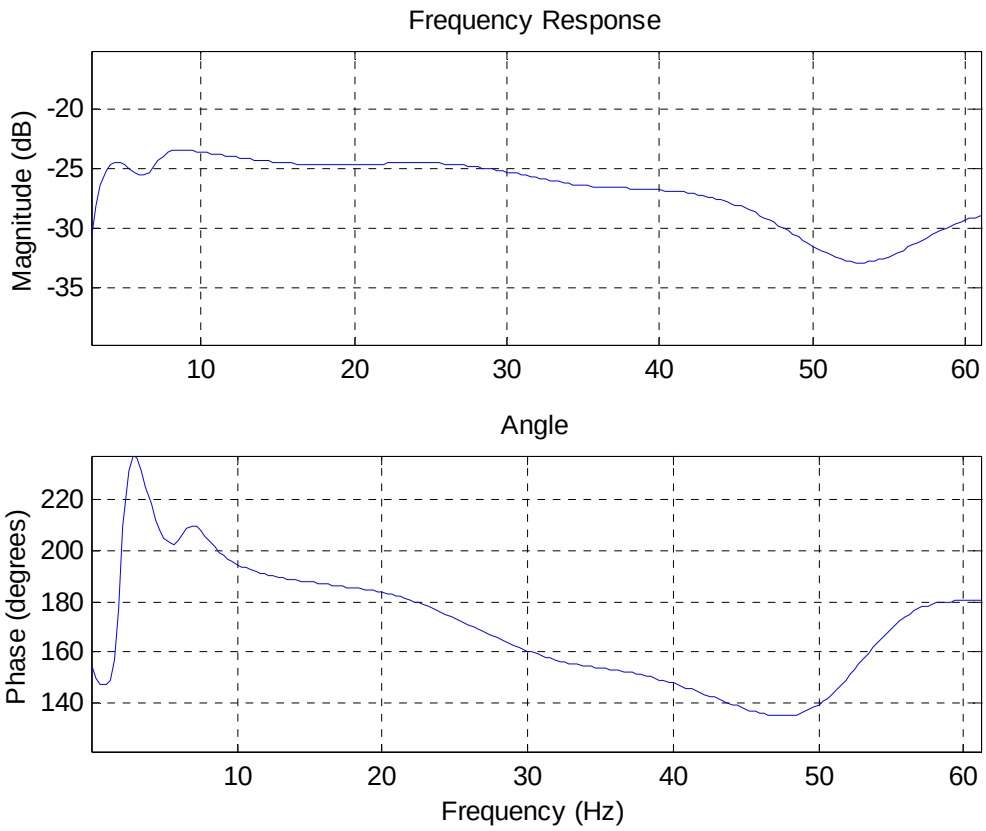


Figure 27. Sample frequency response for the viscoelastic-aluminum foam composite determined during the second test using the impact hammer test.

The Nyquist plot and phase diagram indicate that a natural frequency exists at 28.19 Hz, but the half power bandwidth could not be determined, therefore the damping ratio was not computed. Table 12 is a summary of the natural frequencies and damping ratios determined during the impact hammer test.

| **First test** | | **Second test** | | **Third test** | |
|---|---|---|---|---|---|
| **$\omega_n$ (Hz)** | **$\zeta$ (%)** | **$\omega_n$ (Hz)** | **$\zeta$ (%)** | **$\omega_n$ (Hz)** | **$\zeta$ (%)** |
| 26.32 | ------ | 28.19 | ------ | 25.98 | ------ |
| 80.11 | ------ | 78.94 | 24.62 | 79.37 | 22.75 |

Table 12. Natural frequencies and damping ratios of the viscoelastic-porous aluminum composite using the impact hammer test

Only two damping ratios could be determined because more than half of the frequency plots exhibited characteristics such as figure 27.

## C. RANDOM NOISE

The constrained viscoelastic layer technique appears to increase the damping of the aluminum while maintaining a lightweight and stiff material. The random noise test was used to further investigate the damping properties of the constrained viscoelastic layer technique. The test was conducted for an eighth-inch aluminum plate, a quarter-inch aluminum plate, a 10-ppi quarter-inch 6101 aluminum alloy foam, and 10-ppi half-inch 6101 aluminum alloy foam. The tests were conducted with no constraining layer, with a constraining layer applied to one side of the material, and a constraining layer on both sides of the material for a frequency span of 0 to 1000 Hz. The force gage located in the shaker was used as the input signal, while the accelerometer located in the shaker was used as the output signal.

### 1. Eighth-Inch Aluminum Plate

Both solid aluminum plates were 1 ft by 1 ft plates. Figure 28 is a sample frequency response of the eighth-inch aluminum plate.

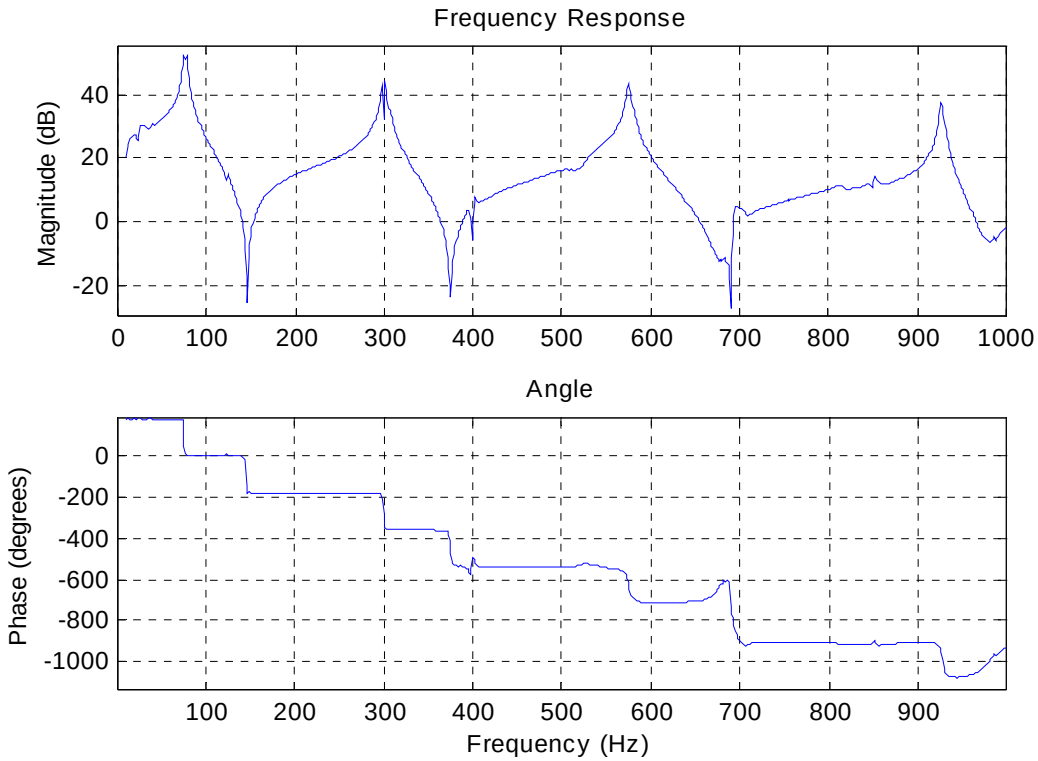


Figure 28. Sample frequency response for the eighth-inch aluminum plate determined during the random noise test

The natural frequencies and damping ratios determined in the test are located in table 13.

| Bare | | 1 side | | Both sides | |
|---|---|---|---|---|---|
| $\omega_n$ (Hz) | $\zeta$ (%) | $\omega_n$ (Hz) | $\zeta$ (%) | $\omega_n$ (Hz) | $\zeta$ (%) |
| 76.00 | 0.33 | 76.34 | 0.92 | 75.44 | 1.33 |
| 300.00 | 0.19 | 302.36 | 0.99 | 297.13 | 1.63 |
| 575.62 | 0.32 | 585.20 | 1.06 | 574.94 | 1.99 |
| 927.87 | 0.16 | 926.88 | 0.96 | 912.88 | 1.29 |

Table 13. Natural frequencies and damping ratios of the eighth-inch aluminum using the random noise test

The damping ratio increased as more constraining layers were added. The damping ratio increased to a maximum value of 1.99 % for the constrained viscoelastic layer applied to both sides of the aluminum plate, which is considerably less than the maximum damping ratio of 22.15 % for the 10-ppi quarter-inch 6101 aluminum alloy foam. Figure 29 shows the trend of the damping ratios and natural frequencies of the eighth-inch aluminum plate.

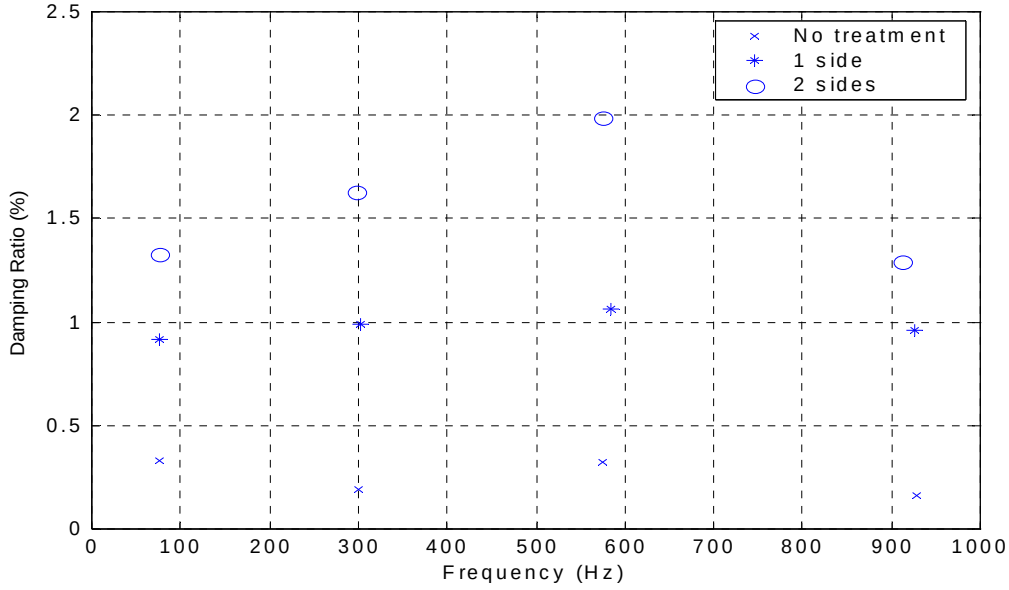


Figure 29. Comparison of the damping ratios and natural frequencies for the eighth-inch aluminum using the random noise test

The constrained viscoelastic layer for the eighth-inch aluminum plate was more effective when applied to both sides of the material than being applied to one side of the material.

### 2. Quarter-Inch Aluminum Plate

The same tests used for the eighth-inch aluminum plate were conducted for the quarter-inch aluminum. A sample frequency plot for the quarter-inch aluminum can be found in figure 30.

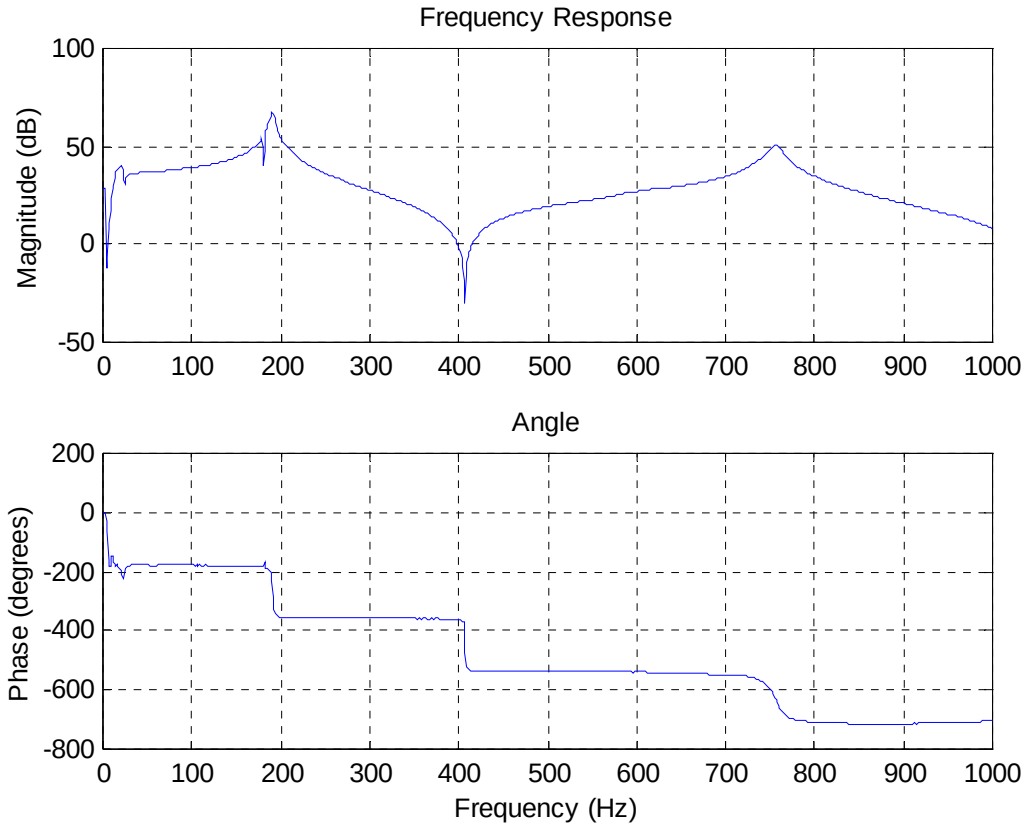


Figure 30. Sample frequency response determined during the random noise test for the quarter-inch aluminum plate with a constraining layer on one side

Figure 30 shows that the quarter-inch aluminum has only 2 natural frequencies in the 0 to 1000 Hz frequency span when treated with a single constraining layer on one side. A summary of the damping ratios and natural frequencies can be found in table 14.

| Bare | | 1 side | | Both sides | |
|---|---|---|---|---|---|
| $\omega_n$ (Hz) | $\zeta$ (%) | $\omega_n$ (Hz) | $\zeta$ (%) | $\omega_n$ (Hz) | $\zeta$ (%) |
| 195.00 | 0.42 | 188.70 | 0.53 | 185.69 | 0.66 |
| 762.00 | 0.13 | 755.00 | 1.03 | 735.81 | 1.40 |

Table 14. Natural frequencies and damping ratios of the quarter-inch aluminum using the random noise test

The constrained viscoelastic layer technique to increase damping had less effect for the quarter-inch aluminum plate than it did for the eighth-inch aluminum plate and the 10-ppi quarter-inch 6101 aluminum alloy foam. The damping ratio achieved a maximum value of 1.40 % when the constrained viscoelastic layer was applied to both sides of the quarter-inch aluminum plate.

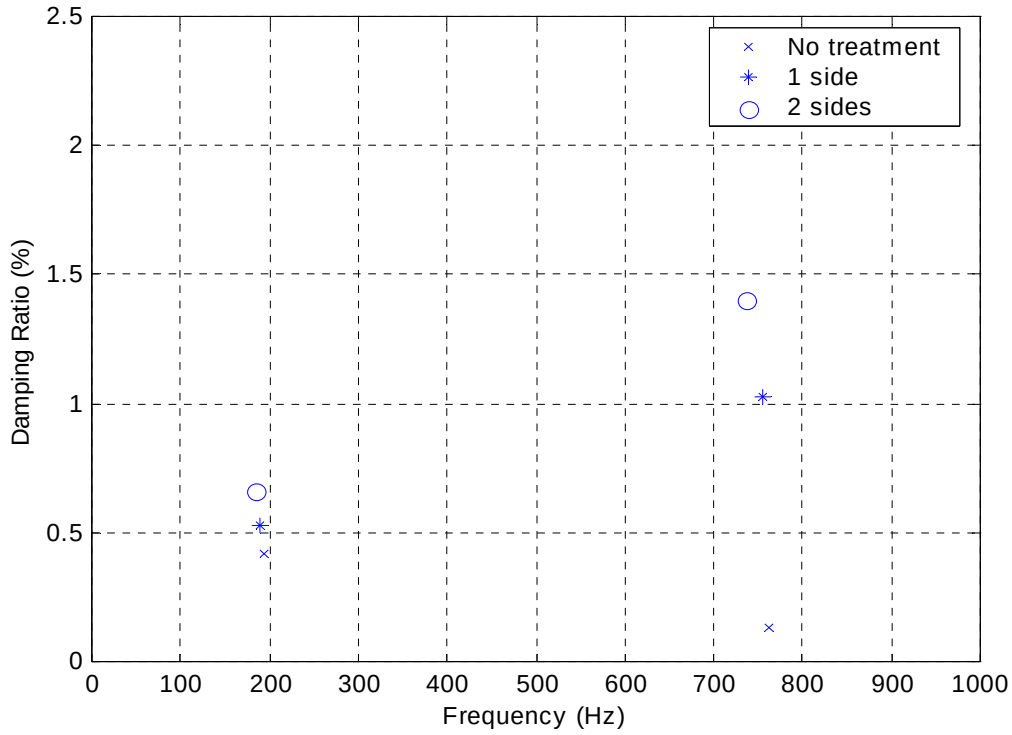


Figure 31. Comparison of the damping ratios and natural frequencies for the quarter-inch aluminum using the random noise test

From figure 31, the constrained viscoelastic layer had little effect on the damping ratio for the first mode of the quarter-inch aluminum plate.

### 3. 10-ppi Quarter-Inch 6101 Aluminum Alloy Foam

Initial tests of the 10-ppi quarter-inch 6101 aluminum alloy foam indicate the constrained viscoelastic layer had a greater effect in increasing the damping of the 10-ppi quarter-inch 6101 aluminum alloy foam than the two solid aluminum cases. Figure 32 is a sample frequency response for the 10-ppi quarter-inch 6101 aluminum alloy foam determined by the random noise test.

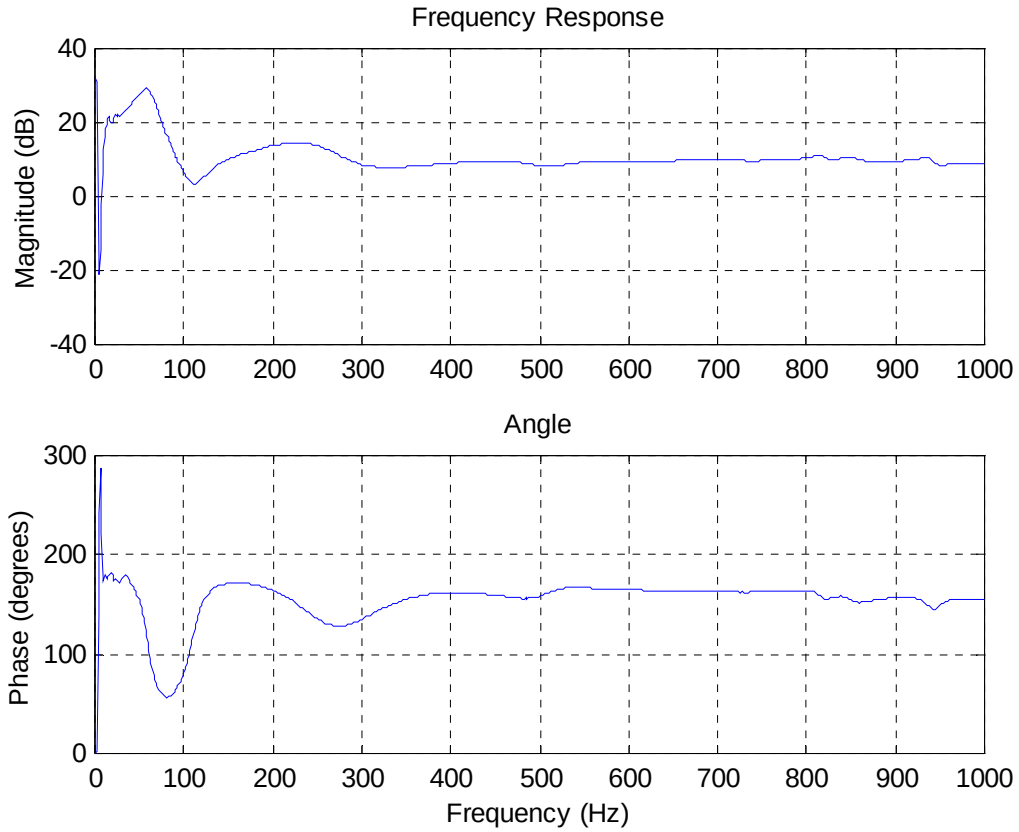


Figure 32. Sample frequency response determined during the random noise test for the 10-ppi quarter-inch 6101 aluminum alloy foam with a constraining layer on both sides

Since the frequency span was increased for the random noise test, there were more natural frequencies and damping ratios determined than in the previous tests. Table 15 is a summary of the natural frequencies and damping ratios determined using the random noise test.

| Bare | | 1 side | | Both sides | |
|---|---|---|---|---|---|
| $\omega_n$ (Hz) | $\zeta$ (%) | $\omega_n$ (Hz) | $\zeta$ (%) | $\omega_n$ (Hz) | $\zeta$ (%) |
| 21.94 | 1.42 | 40.812 | 8.73 | 55.94 | 18.38 |
| 22.75 | 1.33 | 164.50 | 14.97 | 227.50 | 23.85 |
| 29.69 | 0.87 | 322.85 | 17.33 | 814.38 | ------ |
| 51.56 | 0.67 | 542.38 | ------ | 846.94 | ------ |
| 230.06 | 0.27 | 809.49 | ------ | ------- | ------- |
| 270.31 | ------ | 843.09 | ------ | ------ | ------ |
| 276.50 | ------ | 927.50 | ------ | ------ | ------ |
| 281.75 | ------ | ------ | ------ | ------ | ------ |
| 309.88 | ------ | ------ | ------ | ------ | ------ |
| 316.75 | ------ | ------ | ------ | ------ | ------ |
| 347.75 | 0.12 | ------ | ------ | ------ | ------ |
| 378.87 | ------ | ------ | ------ | ------ | ------ |
| 414.00 | ------ | ------ | ------ | ------ | ------ |
| 465.62 | 0.36 | ------ | ------ | ------ | ------ |
| 470.87 | ------ | ------ | ------ | ------ | ------ |
| 480.75 | 0.43 | ------ | ------ | ------ | ------ |
| 491.37 | 0.73 | ------ | ------ | ------ | ------ |
| 500.87 | 0.42 | ------ | ------ | ------ | ------ |
| 511.37 | 2.64 | ------ | ------ | ------ | ------ |
| 598.12 | 0.17 | ------ | ------ | ------ | ------ |
| 640.50 | ------ | ------ | ------ | ------ | ------ |
| 651.50 | ------ | ------ | ------ | ------ | ------ |
| 657.37 | ------ | ------ | ------ | ------ | ------ |
| 668.37 | 0.16 | ------ | ------ | ------ | ------ |
| 683.75 | ------ | ------ | ------ | ------ | ------ |
| 706.00 | ------ | ------ | ------ | ------ | ------ |
| 719.87 | ------ | ------ | ------ | ------ | ------ |
| 745.87 | 0.12 | ------ | ------ | ------ | ------ |
| 804.12 | ------ | ------ | ------ | ------ | ------ |
| 836.25 | ------ | ------ | ------ | ------ | ------ |
| 845.25 | ------ | ------ | ------ | ------ | ------ |
| 933.25 | ------ | ------ | ------ | ------ | ------ |
| 910.25 | ------ | ------ | ------ | ------ | ------ |

Table 15. Natural frequencies and damping ratios of the 10-ppi quarter-inch 6101 aluminum alloy foam using the random noise test

Many of the damping ratios could not be calculated because of interval between natural frequencies was small. The frequency span for one natural frequency often spanned far enough to include other natural frequency, therefore preventing any accurate calculation of the damping ratio using the half-power point method.

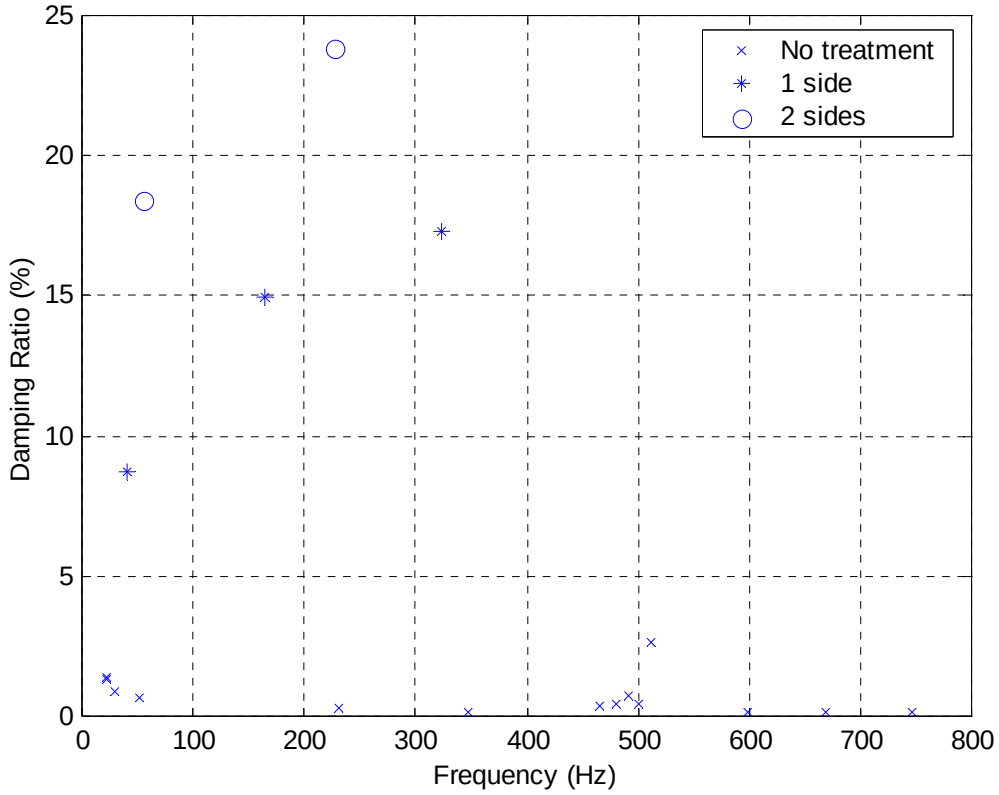


Figure 33. Comparison of the damping ratios and natural frequencies for 10-ppi quarter-inch 6101 aluminum alloy foam using the random noise test

The damping ratio change for the 10-ppi quarter-inch 6101 aluminum alloy foam was greater than the damping ratio increase for both aluminum plates. The random noise test determined a maximum damping ratio of 23.85 % for the constrained viscoelastic layer applied to both sides of the 10-ppi quarter-inch 6101 aluminum alloy foam. The maximum damping ratio value corresponds closely with the maximum damping ratio value determined by the swept sine test (22.14%).

#### 4. 10-ppi Half-Inch 6101 Aluminum Alloy Foam

The 10-ppi half-inch 6101 aluminum alloy foam underwent the same setup and test procedure for the random noise test as the aluminum plates and 10-ppi quarter-inch 6101 aluminum alloy foam. A sample frequency response for the random noise test can be found in figure 34.

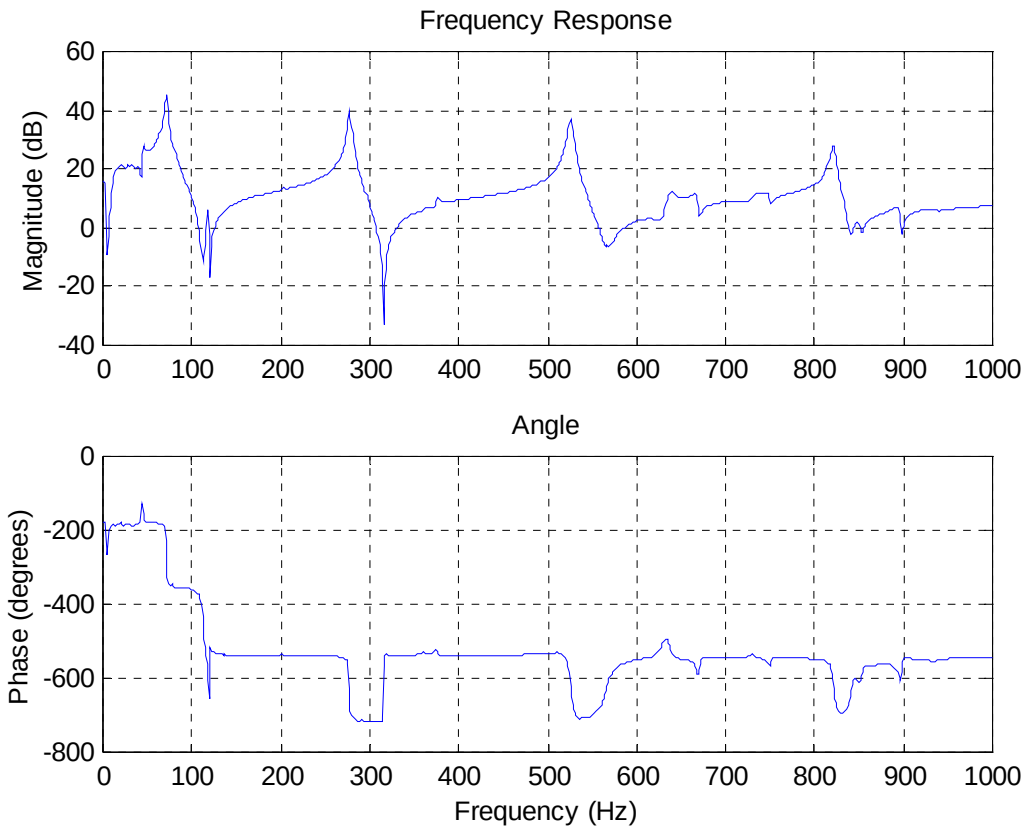


Figure 34. Sample frequency response determined during the random noise test for the half-inch porous aluminum with no treatment

The results of the random noise test is summarized in table 16.

| Bare | | 1 side | | Both sides | |
|---|---|---|---|---|---|
| $\omega_n$ (Hz) | $\zeta$ (%) | $\omega_n$ (Hz) | $\zeta$ (%) | $\omega_n$ (Hz) | $\zeta$ (%) |
| 70.00 | 0.64 | 89.75 | 8.81 | 109.37 | 16.17 |
| 78.20 | 0.70 | 355.50 | 10.32 | 429.50 | 16.76 |
| 117.55 | 0.32 | 647.00 | 10.21 | 847.66 | 12.37 |
| 276.55 | 0.27 | ------ | ------ | ------ | ------ |
| 525.95 | 0.28 | ------ | ------ | ------ | ------ |
| 666.20 | ------ | ------ | ------ | ------ | ------ |
| 821.60 | 0.26 | ------ | ------ | ------ | ------ |
| 895.75 | 0.70 | ------ | ------ | ------ | ------ |

Table 16. Natural frequencies and damping ratios of the 10 ppi half-inch 6101 aluminum alloy foam using the random noise test

The damping ratio increase for the 10 ppi half-inch 6101 aluminum alloy foam was larger than the damping ratio increases for the solid aluminum plate cases but not as large as for the case of the 10-ppi quarter-inch 6101 aluminum alloy foam. The maximum

damping ratio achieved for the 10-ppi half-inch 6101 aluminum alloy foam was 16.76 % for the constrained viscoelastic layer applied to both sides of the aluminum foam.

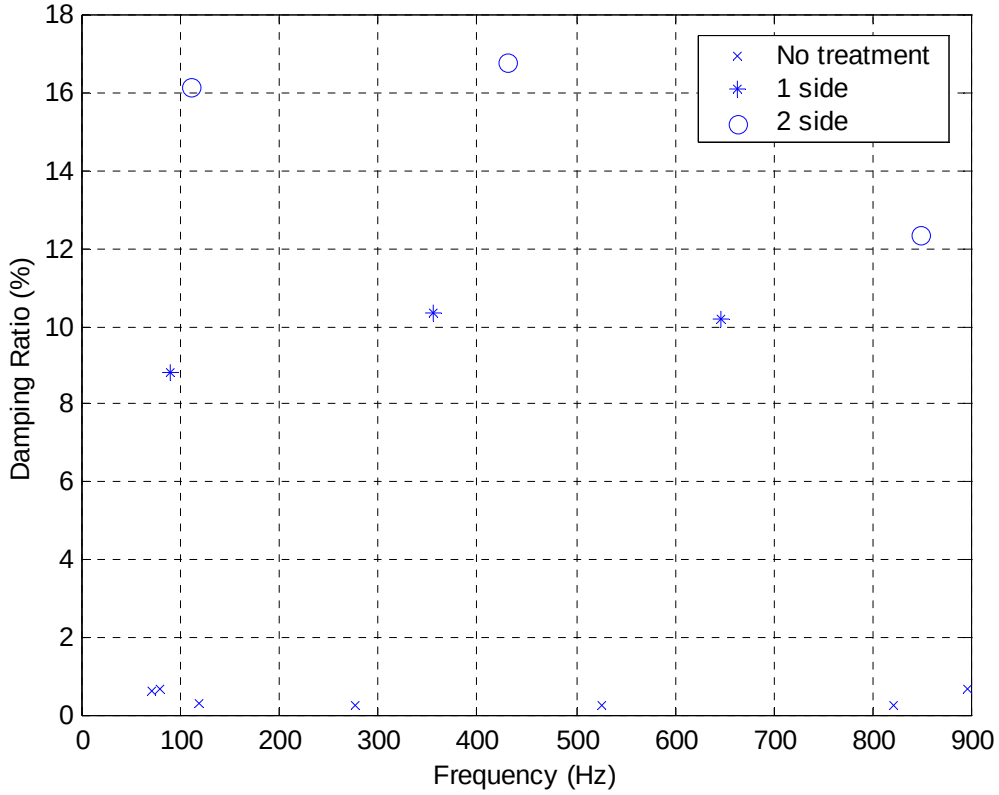


Figure 35. Comparison of the damping ratios and natural frequencies for the 10 ppi half-inch 6101 aluminum alloy foam using the random noise test

THIS PAGE INTENTIONALLY LEFT BLANK

# V. TEST COMPARISONS

Figure 36 compares the results of the damping ratios and natural frequencies for the 10-ppi quarter-inch 6101 aluminum alloy foam using the swept sine, impact hammer and random noise tests.

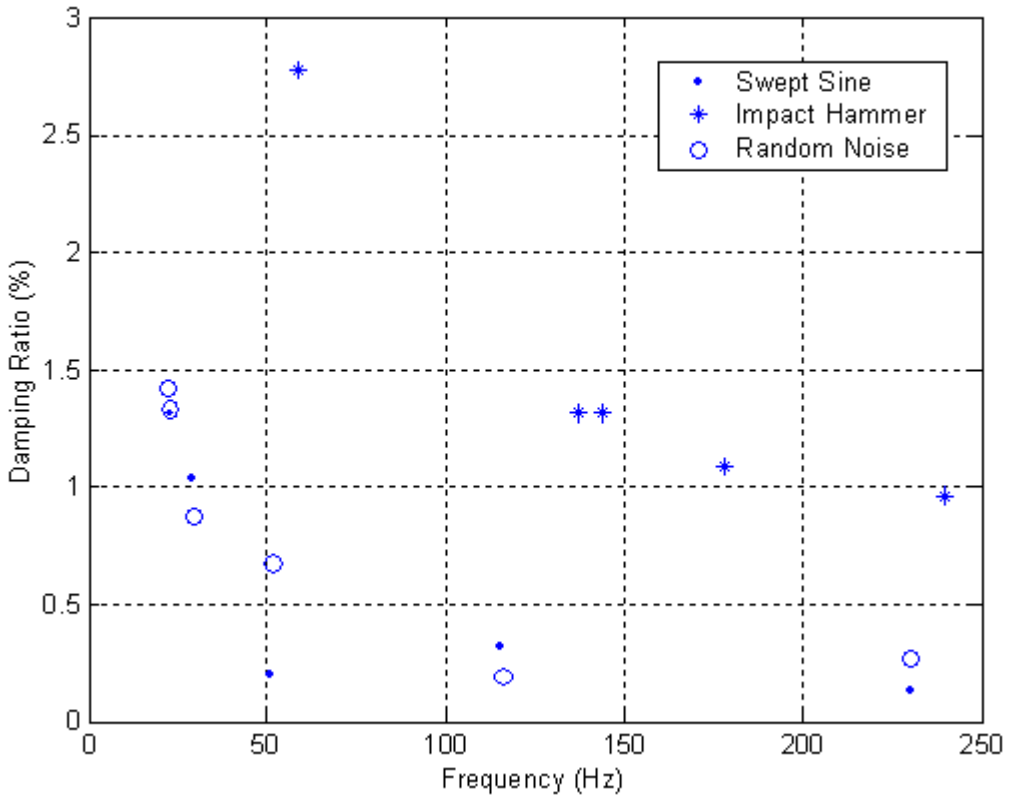


Figure 36. Natural frequencies and damping ratios for the 10-ppi quarter-inch 6101 aluminum alloy foam using the swept sine, impact hammer and the random noise tests

From figure 36, the natural frequencies and damping ratios determined using the swept sine and the random noise test correspond well with each other, while the damping ratios determined by the impact hammer test are consistently higher than those determined with the swept sine and random noise tests. The damping ratios and natural frequencies determined by the swept sine and random noise test are considered more accurate than the impact hammer test because of the problems associated with using the impact hammer test. The pores in the 10-ppi quarter-inch 6101 aluminum alloy foam

made striking the surface with the modal hammer inconsistent. The impact hammer test was therefore not an effective way to determine the vibration properties of the aluminum foam.

Figure 37 shows the damping ratios for one constrained viscoelastic layer applied to both sides of the material determined in the random noise tests versus the weight of the base material.

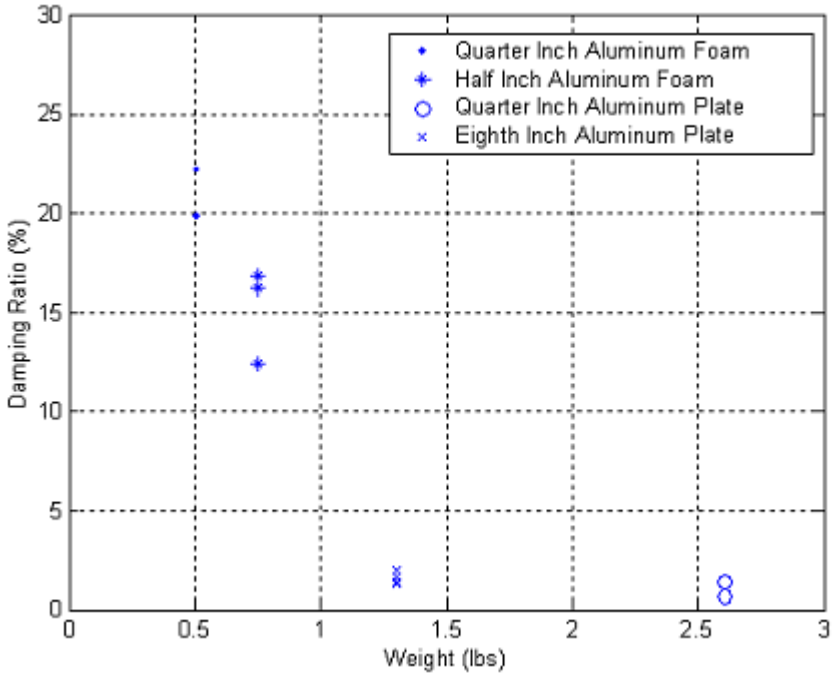


Figure 37. Damping ratios for one constrained viscoelastic layer applied to both sides of the material determined by the random noise test versus the weight of the base material

The test shows the constrained viscoelastic layer produced higher damping ratios for lighter materials. It is still unknown if the correlation of the damping ratio to base material weight is linear because of the different material structures between the solid aluminum plates and the 10 ppi aluminum alloy foams.

Figure 38 illustrates the effectiveness of each of the damping treatments performed of the 10-ppi quarter-inch 6101 aluminum alloy foam.

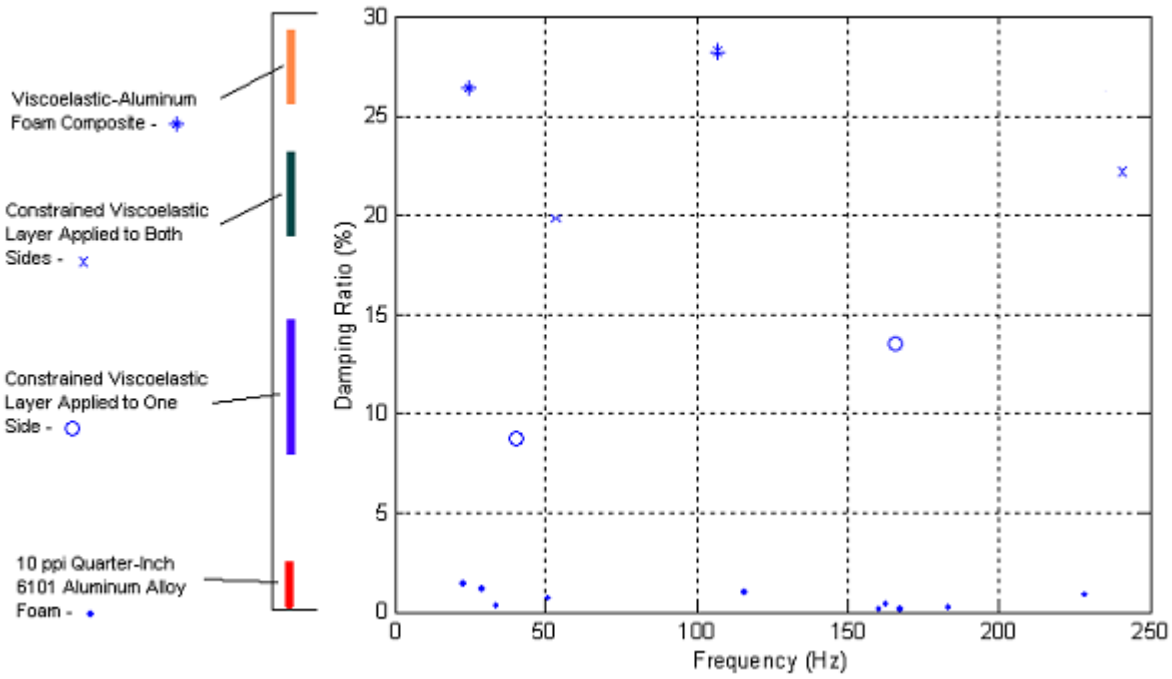


Figure 38. Comparison of the effectiveness of the damping treatments performed on the 10 ppi quarter-inch 6101 aluminum alloy foam

Figure 28 indicates the viscoelastic-aluminum foam composite was the most effective in increasing the damping ratio of the 10-ppi quarter-inch 6101 aluminum alloy foam. The drawback of using the viscoelastic-aluminum foam composite was the increase in the overall weight of the material and the loss of stiffness of the 10-ppi quarter-inch 6101 aluminum alloy foam. The constrained viscoelastic layer applied to both sides of the 10-ppi quarter-inch 6101 aluminum alloy foam had the next highest increase in the damping ratio. Although the damping ratio increase for the constrained viscoelastic layer applied to both sides of the aluminum foam was not as high as the viscoelastic-aluminum foam composite, the aluminum foam stiffness was not lost and the weight of the aluminum foam with the constrained viscoelastic layer applied to both sides was 1.67 times less than the weight of the viscoelastic-aluminum foam composite.

THIS PAGE INTENTIONALLY LEFT BLANK

# VI. CONCLUSIONS AND RECOMMENDATIONS

The viscoelastic-aluminum composite was the most effective in increasing the damping ratio of the aluminum foam. The drawback with the viscoelastic-aluminum composite was the loss of stiffness and the large increase in overall weight. The constrained layer applied to both sides of the 10-ppi quarter-inch 6101 aluminum alloy foam did not increase the damping ratio as high as the viscoelastic-aluminum composite, but the constrained layer applied to both sides of the 10-ppi quarter-inch 6101 aluminum alloy foam was more stiff and weighed 1.67 times less than the viscoelastic-aluminum composite.

The constrained viscoelastic layer was more effective in increasing the damping of the 10-ppi quarter-inch 6101 aluminum alloy foam when multiple layers were applied. The drawback of adding more layers was the significant increase in the weight of the structure. The constrained viscoelastic layers were also more effective when applied to both sides of the material than applying the constrained viscoelastic layer to one side of the material.

Because of the large increase in the damping ratio, the low overall weight, and high stiffness, the constrained viscoelastic layer applied to both sides of the 10-ppi quarter-inch 6101 aluminum alloy foam is more suited for vibration reduction applications were weight is a factor. The viscoelastic-aluminum composite is more suited for applications were weight is not a factor, such as large machinery foundations.

Further research of the acoustic noise reduction properties of the aluminum foam is needed to apply an accurate assessment in the role the material can play as a passive noise reduction material. A test can include the construction of an aluminum foam cylindrical shell. Inside the shell, a speaker would be placed to simulate the noise of a mechanical device. Microphones aligned outside of the cylinder would pick up the level of noise radiated through the cylinder. The test would be conducted using the bare aluminum foam cylindrical shell and then with the damping treatments. Also an underwater assessment of the noise radiation could be conducted to determine the effectiveness of the damping treatments to reduce underwater radiated noise.

THIS PAGE INTENTIONALLY LEFT BLANK

# LIST OF REFERENCES


1. Yang, C.C. and Nakae, H., "Foaming Characteristics Control During Production of Aluminum Alloy Foam," Journal of Alloys and Compounds, Vol. 313, 2000.

2. Sigmund, O. "Materials with Prescribed Constitutive Parameters: An Inverse Homogenization Problem," International Journal of Solids and Structures, Vol. 31, 1994.

3. Bendoe, M.P., Kikuchi, N., "Generating Optimal Topologies in Structural Design Using a Homogenization Method," Computer Methods in Applied Mechanics and Engineering, Vol. 71, 1988.

4. Yeong-Moo Yi, Sang-Hoon Park, Sung-Kie Youn, "Design of Microstructures of Viscoelastic Composites for Optimal Damping Characteristics," International Journal of Solids and Structures, Vol. 37, 2000.

5. Johnson, C.D. and Kienholz, D. A., "Finite Element Prediction of Damping in Structures With Constrained Viscoelastic Layers,' AIAA Journal, Vol. 20, 1982."

6. Bateman, M.J., Constrained Viscoelastic Layer Damping of Thick Aluminum Plates: Design, Analysis, and Testing, M.S. Thesis, U.S. Naval Postgraduate School, Monterey, California, March 1990.

7. Thomson W.T. and M.D. Dahleh, Theory of Vibration With Applications, 5th Ed., Prentice-Hall Inc, 1998.

8. ERG Aerospace Co., www.ergaerospace.com, ERG Aerospace Co.

9. Diamant Coating Systems, Ltd., Diamant Dichtol, Diamant Coating Systems, Ltd.

10. Hewlett-Packard Co., 3562A Dynamic Signal Analyzer Operating Manual, Hewlett-Packard Co., 1985.

11. Wilcoxon Research, Instruction Manual, Model F7/F4 Piezoelectric /Electromagnetic Vibration Generator System, Wilcoxon Research, 1985.

THIS PAGE INTENTIONALLY LEFT BLANK

# INITIAL DISTRIBUTION LIST

1. Defense Technical Information Center
   8725 John J. Kingman Rd., Ste 0944
   Ft. Belvoir, Va 22060-6218

2. Dudley Knox Library
   Naval Postgraduate School
   411 Dyer Rd.
   Monterey, Ca 93943-5101

3. Professor Young W. Kwon, Code ME
   Department of Mechanical Engineering
   Naval Postgraduate School
   Monterey, CA 93943

4. Professor Young S. Shin, Code ME
   Department of Mechanical Engineering
   Naval Postgraduate School
   Monterey, CA 93943

5. Naval/Mechanical Engineering Curricular Office
   Department of Mechanical Engineering
   Naval Postgraduate School
   Monterey, CA 93943